CARPATHIAN JOURNAL OF FOOD SCIENCE AND TECHNOLOGY

journal homepage: **http://chimie-biologie.ubm.ro/carpathian_journal/index.html**

OPEN ACCESS

CC BY SA

Research article

SPRAY DRYING ENCAPSULATION OF BIOACTIVE COMPOUNDS FROM *RED CARDINAL* GRAPE POMACE EXTRACTED USING DEEP EUTECTIC SOLVENT

Thao Thi Thanh Nguyen[1], Hien Minh Nguyen[1], Tuyen Chan Kha[1]✉

[1] *Department of Food Microbiology and Product Development, Faculty of Chemical Engineering and Food Technology, Nong Lam University, Ho Chi Minh City, Vietnam*

✉*Tuyen Chan Kha, ORCID Number: 0000-0003-0632-7197, E-mail: khachantuyen@hcmuaf.edu.vn*

https://doi.org/10.34302/crpjfst/ARZF1070

Article history:
Received:
February 2nd 2026
Accepted:
July 27th 2026
Published:
November 23th 2026

Keywords
Bioactive compounds;
Deep eutectic solvent;
Encapsulation,
Red Cardinal,
Spray drying.

Abstract

The deep eutectic solvent (DES) extract of bioactive compounds from *Red Cardinal* grape pomace exhibited significant antioxidant and antimicrobial properties. Encapsulation is a promising technology to enhance the stability and prolong the shelf life of these bioactive compounds by protecting them from environmental degradation. This research investigated the effects of various parameters on the encapsulation of bioactive compounds in DES extract from *Red Cardinal* grape pomace. Key independent variables included wall material type, core-to-wall material ratio, wall material blend ratio, homogenization speed and duration, inlet air temperature, and feed flow rate. Encapsulation yield, encapsulation efficiency, water activity, and powder particle morphology were evaluated, while X-ray diffraction, differential scanning calorimetry, and Fourier-transform infrared spectroscopy were employed to determine the most suitable encapsulation conditions. The results demonstrated that spray drying is an effective method for encapsulating DES-extracted bioactive compounds. The best spray drying conditions were identified as a maltodextrin-to-gum arabic ratio of 2:1 (w/w), a core-to-wall material ratio of 1:4 (w/w), homogenization at 10,800 rpm for 10 min, an inlet air temperature of 160 °C, and a feed flow rate of 35 mL/min. The resulting microencapsulated powder showed strong potential for applications in the food and pharmaceutical industries.

1. Introduction

The valorization of agro-industrial byproducts has garnered significant interest in recent years, particularly in the context of sustainable resource utilization and circular economy initiatives. Among these byproducts, grape pomace, generated during winemaking and juice processing, is a rich source of bioactive compounds such as polyphenols, flavonoids, and proanthocyanidins. These compounds exhibit potent antioxidant, antimicrobial, and anti-inflammatory activities, rendering them valuable for applications in the food and pharmaceutical industries (Peixoto *et al.*, 2018).

Conventional extraction of bioactive compounds from plant matrices typically relies

on organic solvents, which raise environmental and safety concerns. In this regard, DESs, comprising a hydrogen bond acceptor (e.g., choline chloride) and a hydrogen bond donor (e.g., lactic acid), have emerged as a sustainable alternative. DESs offer several advantages, including biodegradability, low toxicity, and ease of preparation (Dai *et al.*, 2013). Recent studies have demonstrated the efficacy of choline chloride-lactic acid-based DES in extracting phenolic-rich fractions from *Red Cardinal* grape pomace, highlighting their potential as a green extraction medium (Nguyen *et al.*, 2025). Nevertheless, the DES-extracted bioactives remain susceptible to degradation, necessitating stabilization strategies to preserve their functional integrity during processing and storage.

Encapsulation of grape pomace bioactive compounds represents a promising strategy to overcome their inherent instability and enhance their applicability in functional products. Microencapsulation, particularly via spray drying, is widely employed to improve the stability, bioavailability, and controlled release of sensitive bioactive compounds (López-Astorga *et al.*, 2025; Tolun *et al.*, 2016). In addition, spray drying offers advantages such as rapid drying and scalability. In recent years, significant progress has been made in wall material selection, process optimization, and understanding of release mechanisms contributing to enhanced stability and functionality (López-Astorga *et al.*, 2025). However, microencapsulation of DES-extracted compounds remains limited. The distinct physicochemical properties of DESs, such as higher viscosity, lower volatility, and variable pH compared to conventional solvents, necessitate a tailored approach to spray drying. Combinations of common wall materials such as maltodextrin (MD), gum arabic (GA), modified starches (MS), soy protein isolate (SPI), and whey protein isolate (WPI) often yield higher microencapsulation efficiency (Xiao *et al.*, 2022), making the ratio between wall components a critical factor. Additionally, inlet air temperatures ranging from 100 to 180 °C are typically applied to preserve heat-sensitive compounds during spray drying (Jafari *et al.*, 2023). The core-to-wall material ratio must also be determined to ensure adequate encapsulation and minimize compound loss.

This research aimed to investigate the key factors affecting the spray drying encapsulation DES-extracted of bioactive compounds from *Red Cardinal* grape pomace. Specific objectives were to evaluate the effects of wall material composition, core-to-wall ratios, homogenization speed and duration, and spray drying conditions on encapsulation yield, encapsulation efficiency, powder morphology, moisture content, water activity, and the thermal and structural properties of the resulting microcapsules.

2. Materials and methods

2.1. Raw Materials and Chemicals

2.1.1. Raw materials

Raw grape pomace (including skins, stems, and seeds) was collected from Ba Moi Company (Vietnam). Preliminary processing involved removing the stems and seeds, followed by drying the remaining pomace using a heat pump dryer under controlled conditions: air temperature of 35 °C for 12 hours, material loading density of 3 kg/m^2, air velocity of 1.8 m/s, until the moisture content was reduced to below 10%. The dried pomace was then finely ground and sieved through a 0.5 mm mesh to ensure uniform particle size. The resulting powder was packed in light-protective bags and stored at −18 °C until further use.

2.1.2. Chemicals

All chemicals were of analytical grade. Choline chloride, vanillin, and Folin–Ciocalteu reagent were sourced from Himedia (India); lactic acid, sulfuric acid, hydrochloric acid, sodium carbonate, aluminum chloride, and sodium hydroxide from Xilong (China); and sodium nitrite from Guangdong Guanghua (China). Wall materials included maltodextrin (MD; DE 15 – 20) and gum arabic (GA), both purchased from Path Co., Ltd., Vietnam, soy protein isolate (SPI) from Sangdong Yuxin, China, modified starch (MS) from Neo Foodtech Co., Vietnam, and whey protein

isolate (WPI) from Bluetech Ingredients Ltd, Vietnam.

2.2. Methods

2.2.1. Extraction of bioactive compound from grape pomace

The deep eutectic solvent was prepared by mixing choline chloride and lactic acid at a 1:2 (w/w) ratio, with the addition of 20% (w/w) water. The mixture was heated to 80 °C and stirred at 260 rpm for 1.5 hours until a clear, homogeneous solution was obtained. Grape pomace powder was mixed with the DES at a 1:25 (w/w) ratio and stirred at 70 °C for 118 min at 260 rpm under light-protected conditions (Nguyen *et al.*, 2025). The resulting mixture was then centrifuged at 6,000 rpm for 10 min, and the supernatant was collected for subsequent microencapsulation.

2.2.2. Microencapsulation of bioactive compound extract

Wall material solutions were prepared using maltodextrin alone or in combination with other wall materials, including maltodextrin: gum arabic (MD-GA) (1:2, w/w), maltodextrin: modified starch (MD-MS) (10:1, w/w), maltodextrin: soy protein isolate (MD-SPI) (7:1, w/w), and maltodextrin: whey protein isolate (MD-WPI) (9:1, w/w) (Cano-Higuita *et al.*, 2015; Nguyen *et al.*, 2017; Rosenberg *et al.*, 2016; Shi *et al.*, 2013). The wall material solution had a fixed dry matter concentration of 40%. The ratio of maltodextrin to the other wall materials was further evaluated at 1:2, 1:1, 2:1, and 3:1 (w/w). Wall material was mixed with distilled water and incubated in a water bath (GFL 1003, Lauda, Germany) at 60 °C for approximately 120 min to form a homogeneous mixture. The extract and wall material solution were then mixed at different core-to-wall ratios (1:3, 1:4, 1:5, and 1:6, w/w dry weight). The mixtures were homogenized using a SciLab SHG-15A homogenizer (Korea) at speeds of 8,100 rpm or 10,800 rpm for 5, 10, or 15 min. The homogenized solutions were spray-dried using an L-8i spray dryer (Ohkawara Kakohki Co. Ltd., Japan) at inlet air temperatures ranging from 140 – 180 °C and feed flow rates between 15 – 45 mL/min. The atomizer speed was maintained at 18,000 rpm, and the pressure at 1.55 kPa. The resulting powder was collected and stored in light-protective bags for further analysis.

2.2.3. Determination of Total Phenolic Content (TPC), Total Saponin Content (TSC), and Proanthocyanidin Content (PAC)

TPC was measured using UV–Vis spectrophotometric method (Škulcova *et al.*, 2018). Briefly, 0.5 mL of diluted sample was mixed with 0.5 mL of 10% Folin–Ciocalteu reagent. After 5 min, 2.5 mL of 20% sodium carbonate was added. The mixture was incubated at ambient temperature for 90 min, and absorbance was recorded at 765 nm. Results were expressed as mg gallic acid equivalents per gram dry weight (mg GAE/g DW).

For TSC, 0.3 mL of diluted sample was mixed with 0.3 mL of 8% vanillin and 3 mL of 72% sulfuric acid. The mixture was incubated at 60 °C for 15 min, cooled for 10 min, and the absorbance was measured at 560 nm. TSC was expressed as mg aescin equivalents per gram dry weight (mg AE/g DW) (Tan *et al.*, 2014).

PAC was determined by reacting 0.5 mL of sample with 0.3 mL of 4% vanillin and 1.5 mL of hydrochloric acid. After incubation for 15 min at ambient temperature, the absorbance was measured at 500 nm. PAC was expressed as mg catechin equivalents per gram dry weight (mg CE/g DW) (Li *et al.*, 2006).

2.2.4. Determination of encapsulation yield and encapsulation efficiency

The encapsulation yield (EY, %) was calculated based on the TPC, TSC, and PAC in the spray-dried powders relative to those in the initial feed solution. The EY reflects the retention of bioactive compounds after the spray drying process and was calculated using the following formula:

$$\text{EY (\%)} = \frac{\text{Content of bioactive compounds in encapsulated powder}}{\text{Content of bioactive compounds in feed solution}} \times 100 \quad (1)$$

Encapsulation efficiency (EE, %) represents the percentage of bioactive compounds successfully encapsulated within the microparticles, excluding those adsorbed on the surface (Perković *et al.*, 2024; Vu *et al.*, 2023). Specifically, 1 g of encapsulated powder was mixed with 3 mL of 80% (w/v) ethanol in a test tube, gently shaken, and left at ambient temperature for 1 min to extract surface compounds. The mixture was then filtered using a 0.45 µm PTFE syringe filter, and the filtrate was analyzed for TPC, TSC, and PAC using the spectrophotometric methods. The encapsulation efficiencies in terms of TPC (EE(TPC)), TSC (EE(TSC)), and PAC (EE(PAC)) were calculated using the following equations:

$$\text{EE(TPC)}\ (\%) = \frac{\text{TPC} - \text{SPC}}{\text{TPC}} \times 100 \quad (2)$$

$$\text{EE(TSC)}\ (\%) = \frac{\text{TSC} - \text{SSC}}{\text{TSC}} \times 100 \quad (3)$$

$$\text{EE(PAC)}\ (\%) = \frac{\text{PAC} - \text{SPAC}}{\text{PAC}} \times 100 \quad (4)$$

Where TPC, TSC, and PAC refer to the total contents of polyphenols (mg GAE/g DW), saponins (mg AE/g DW), and proanthocyanidins (mg CE/g DW) in the encapsulated powder, respectively. SPC, SSC, and SPAC refer to the surface contents of TPC (mg GAE/g DW), TSC (mg AE/g DW), and PAC (mg CE/g DW) on the outer surface of the microparticles, respectively.

2.2.5. Determination of moisture content and water activity

The moisture content (MC) of the samples was determined according to AOAC official method 925.45. The water activity of the samples was determined using an Aqualab Series 3 water activity meter (Decagon Devices Inc., USA) at ambient temperature.

2.2.6. Powder particle morphology analysis

The surface morphology of the spray-dried encapsulated powders was determined using a field emission scanning electron microscope (FESEM S4800, Hitachi, Japan). Powder samples were mounted on aluminum stubs using conductive carbon adhesive tape. The E1045 Pt coater (Hitachi, Japan) was used to deposit a thin layer of platinum (Pt) onto the samples. Representative micrographs were taken at different magnifications to visualize the surface morphology.

2.2.7. X-ray Diffraction (XRD) analysis

XRD analysis was conducted using a D2 Phaser Benchtop X-ray Powder Diffractometer (Bruker, Germany), operating at 30 kV and 10 mA. The samples were loaded into a disc sample holder, and X-ray diffraction patterns were recorded using Cu Kα radiation (λ = 0.154060 nm) over a 2θ range of 5° – 40°, at a scanning speed of 4°/min and a step size of 0.02° (Frank *et al.*, 2021). The XRD data were used to evaluate the crystallinity of the encapsulated powders.

2.2.8. Differential scanning calorimetry (DSC) analysis

DSC analysis was performed to assess the thermal properties of the microcapsules. DSC curves were recorded using a DSC300 Caliris Select instrument (NETZSCH, Germany). Approximately 2 mg of each sample was placed in aluminum pans and analyzed under a dynamic nitrogen flow (40 mL/min), with heating from 30 °C to 400 °C at a rate of 10 °C/min (Negrao-Murakami *et al.*, 2016). The DSC system was calibrated in advance using indium as a standard.

2.2.9. Fourier–Transform Infrared (FTIR) Spectroscopy

FTIR spectroscopy was performed using a Cary 630 FTIR spectrometer (Agilent Technologies, USA). Spectra were recorded in the wavenumber range of 650 – 4000 cm^{-1} at a resolution of 4 cm^{-1}, with 32 scans per sample (Janiszewska-Turak *et al.*, 2022). The spectra were used to assess potential chemical interactions between the bioactive compounds and wall materials.

2.2.10. Particle Size Distribution Analysis

The particle size distribution of the microcapsules was determined using an LS 13 320 Particle Size Analyzer (Beckman Coulter, USA). Encapsulated powder particles were dispersed in deionized water and vortexed to

ensure adequate dispersion before measurement. Particle size distribution parameters, including mean, mode, D10, D50, and D90, were recorded.

2.3. Data analysis

The experiments were conducted using either one-factor or two-factor designs, with three repetitions per treatment. Data were statistically analyzed using JMP 13 software. Results are presented as mean ± standard deviation (mean ± SD). Analysis of variance was applied to assess the significance of differences among treatment means. When significant differences were found, the Tukey HSD was used at a 5% significance level ($P \leq 0.05$).

3. Results and discussions

3.1. Effects of wall material types on the encapsulation

The aim was to assess the influence of wall material type on the encapsulation of bioactive compounds extracted from grape pomace and to identify the most suitable material for spray-drying applications. Fixed parameters included a core-to-wall ratio of 1:5 (w/w), homogenization speed of 8,100 rpm for 10 min, inlet air temperature of 170 °C, and feed flow rate of 15 mL/min. The results, presented in Figure 1a, demonstrate significant differences in encapsulation yield depending on the wall material used ($P \leq 0.05$). When MD was used alone, it provided the highest encapsulation yield for TPC and PAC. In contrast, the MD-SPI combination resulted in the lowest encapsulation yields, indicating that SPI may not be suitable for encapsulating these particular compounds under the tested conditions. The combinations of MD with GA, MS, or WPI resulted in moderate encapsulation yields. For TSC, the MD-GA combination exhibited the highest encapsulation yield (82.07 ± 2.42%), suggesting that the favorable interaction between GA and saponins may enhance encapsulation performance during spray drying.

MD alone achieved high encapsulation yield for both TPC and PAC. However, its yield for TSC was relatively lower than that of the MD-GA combination. MD is favored for its advantageous physicochemical properties, including low viscosity, high solubility, and its ability to reduce stickiness in the final powder, all of which contribute to improved microencapsulation performance and product handling (Xiao *et al.*, 2022). In contrast, the combination of MD with SPI resulted in significantly lower encapsulation yield across all three indicators as compared with MD-WPI. Both WPI and SPI were capable of forming protective films around core materials through interactions between phenolic compounds and protein molecules. However, the recovery of phenolics may be compromised by protein denaturation, particularly under high temperatures or at elevated concentrations, which can reduce the availability of native protein structures that interact effectively with polyphenols. Notably, increasing WPI beyond an optimal level may lead to a decline in phenolic recovery (Moreno *et al.*, 2016).

The results presented in Figure 1b demonstrate that encapsulation efficiency varied significantly as a function of wall material type ($P \leq 0.05$). The highest encapsulation efficiencies for TPC, TSC, and PAC were achieved using the MD-GA combination. Although MD alone has been reported to improve encapsulation efficiency (Xiao *et al.*, 2022), the incorporation of GA further increased infeed viscosity and solution stability prior to spray drying, contributing to superior encapsulation performance compared with the use of MD alone.

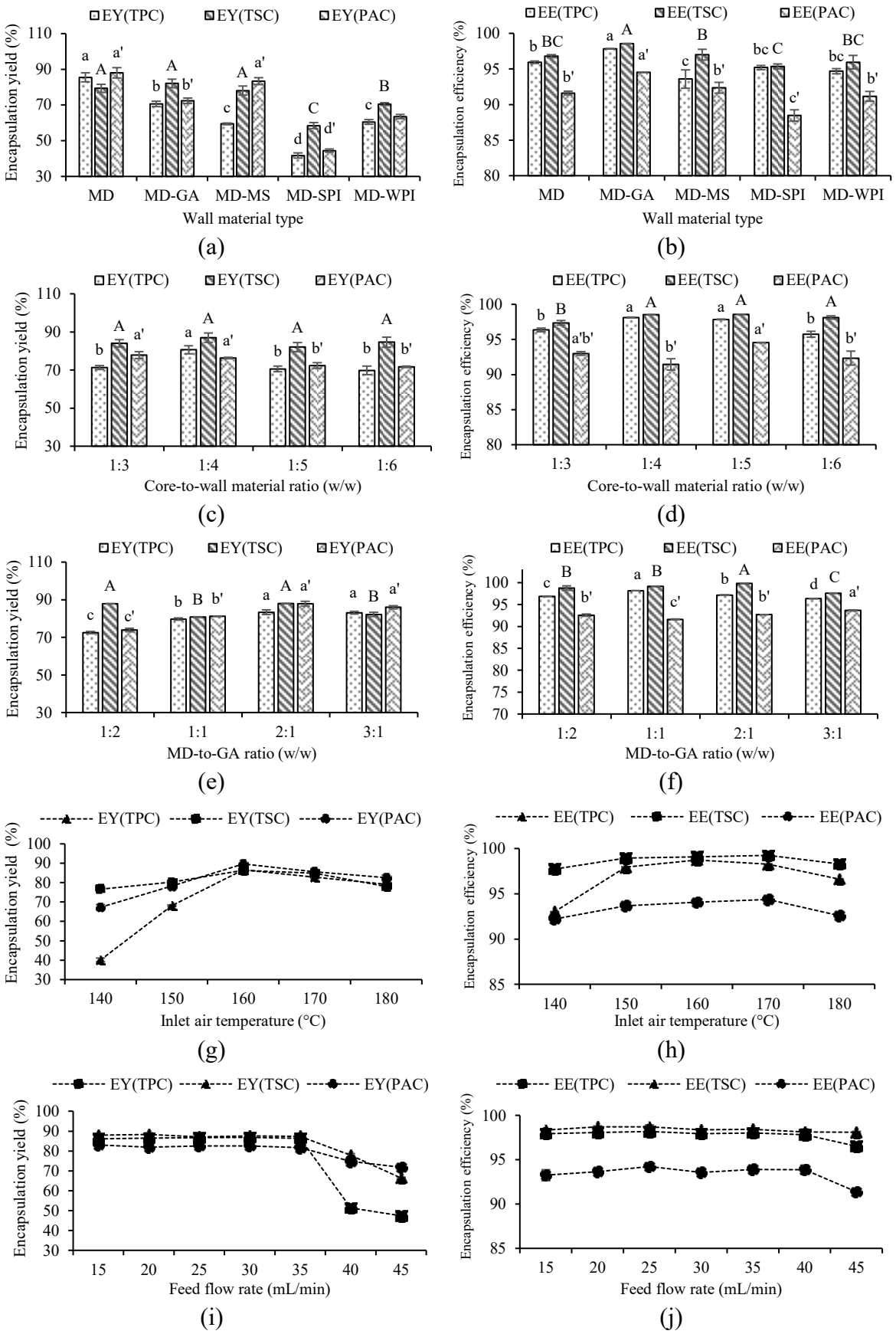

Figure 1. Effects of spray drying conditions on encapsulation yield and encapsulation efficiency

This suggests that GA, known for its excellent film-forming capacity and solubility, significantly enhances the encapsulation efficiency when combined with MD. GA is a natural, branched polysaccharide capable of interacting efficiently with polyphenols, thereby facilitating the formation of a stable encapsulating matrix (Mariod, 2018). In contrast, the MD-SPI formulation exhibited the lowest encapsulation efficiencies for all measured compounds. The remaining wall material combinations showed moderate encapsulation performance.

Moisture content and water activity are two critical parameters that significantly affect the quality, stability, and shelf life of encapsulated powders. Table 1 shows that both parameters varied significantly depending on the type of wall material used ($P \leq 0.05$). Moisture content ranged from 3.04 ± 0.21% in powders encapsulated with MD alone to 6.03 ± 0.52% in those formulated with MD-GA combination. MD, characterized by a relatively linear molecular structure and fewer free hydroxyl groups, showed the lowest water-holding capacity, resulting in significantly reduced moisture content (3.04 ± 0.21%) and water activity (0.149 ± 0.004). In contrast, GA, characterized by a branched structure and a high density of hydroxyl groups, demonstrated strong hydrogen-bonding potential with water molecules (Mariod, 2018). This contributed to higher moisture content (6.03 ± 0.52%) in the MD–GA formulation. WPI, composed mainly of small, hydrophilic proteins such as β-lactoglobulin and α-lactalbumin, binds water in a free form, which is readily removed during spray drying. As a result, the MD-WPI formulation also exhibited low final moisture content (Qi and Onwulata, 2011). Despite these variations, all formulations maintain water activity values below 0.2, a threshold considered critical for microbial stability and ensuring extended shelf life. Notably, although the MD-GA (1:2 w/w) formulation showed the highest moisture content under the fixed spray drying conditions of 170 °C and a feed flow rate of 15 mL/min, the resulting powder remained dry and had low hygroscopicity, with a slower moisture uptake over time compared to other wall material combinations.

Table 1. Influence of spray-drying conditions on the moisture content and water activity of the encapsulated powder

Key independent variables	Samples	Moisture content (%)	Water activity
Wall material type	MD	$3.04^{d} \pm 0.21$	$0.149^{b} \pm 0.004$
	MD-GA	$6.03^{a} \pm 0.49$	$0.192^{a} \pm 0.005$
	MD-MS	$5.20^{ab} \pm 0.78$	$0.182^{ab} \pm 0.017$
	MD-SPI	$4.55^{bc} \pm 0.04$	$0.174^{ab} \pm 0.011$
	MD-WPI	$3.53^{cd} \pm 0.39$	$0.169^{ab} \pm 0.026$
Core-to-wall material ratio (w/w)	1:3	$6.69^{a} \pm 0.52$	$0.132^{b} \pm 0.008$
	1:4	$6.56^{a} \pm 0.15$	$0.141^{b} \pm 0.003$
	1:5	$6.03^{ab} \pm 0.49$	$0.192^{a} \pm 0.005$
	1:6	$4.72^{b} \pm 1.06$	$0.193^{a} \pm 0.011$
MD-to-GA ratio (w/w)	1:2	$6.93^{a} \pm 0.03$	$0.215^{a} \pm 0.005$
	1:1	$5.40^{b} \pm 0.06$	$0.214^{a} \pm 0.003$
	2:1	$4.31^{c} \pm 0.02$	$0.209^{a} \pm 0.003$
	3:1	$3.59^{d} \pm 0.02$	$0.118^{b} \pm 0.007$
Inlet air temperature (°C)	140	$4.86^{a} \pm 0.12$	$0.163^{a} \pm 0.015$
	150	$4.56^{b} \pm 0.15$	$0.171^{a} \pm 0.009$
	160	$4.10^{c} \pm 0.06$	$0.152^{a} \pm 0.026$
	170	$3.97^{cd} \pm 0.05$	$0.145^{a} \pm 0.012$

	180	$3.75^{d} \pm 0.11$	$0.134^{a} \pm 0.011$
Feed flow rate (mL/min)	15	$4.15^{e} \pm 0.14$	$0.131^{a} \pm 0.018$
	20	$4.67^{de} \pm 0.25$	$0.134^{a} \pm 0.010$
	25	$5.24^{cd} \pm 0.06$	$0.136^{a} \pm 0.015$
	30	$5.31^{cd} \pm 0.04$	$0.138^{a} \pm 0.002$
	35	$5.78^{bc} \pm 0.11$	$0.140^{a} \pm 0.015$
	40	$6.22^{b} \pm 0.53$	$0.137^{a} \pm 0.011$
	45	$7.36^{a} \pm 0.12$	$0.125^{a} \pm 0.026$

Distinct superscript letters within same key independent variable and column indicate statistically significant differences ($P \leq 0.05$).

The physicochemical properties of the spray-dried microcapsules, as influenced by different wall materials, were investigated using XRD, FTIR, and DSC analyses, as presented in Figure 2. The XRD patterns (Figure 2a) confirmed that all powder samples revealed predominantly amorphous characteristics. This was evidenced by broad diffraction halos centered around 20° (2θ) and the absence of distinct crystalline peaks. The MD-based formulation displayed a relatively sharper broad peak, suggesting a partially ordered structure compared to other formulations, with the highest crystallinity of 28% among the tested formulations. In contrast, powders produced using combinations of wall materials (MD-GA, MD-MS, MD-SPI, and MD-WPI) showed broader and more diffused halos, indicating a higher degree of amorphization. The formation of an amorphous structure is advantageous in microencapsulation, as it increases matrix viscosity, reduces molecule mobility, and suppresses degradation reactions. This structure effectively protects bioactive compounds by minimizing their exposure to oxygen, moisture, and temperature variations (Xiao *et al.*, 2022). In addition, amorphous encapsulated powders have been reported to exhibit improved bioavailability compared to their crystalline counterparts (Kalajahi and Ghandiha, 2022), underscoring the relevance of wall material selection in functional food applications.

FTIR analysis was performed to identify functional groups and evaluate potential interactions between the core extract and the different wall materials (Figure 2b). In the FTIR spectrum of the extract, an absorption band at approximately 954 cm^{-1} can be associated with vibrations related to the DES system, likely originating from choline chloride. Both the extract and encapsulated powders showed a characteristic band around 1720 cm^{-1}, primarily attributed to the C=O stretching vibration of the carboxyl group, with a major contribution from lactic acid in the DES. Absorption peaks observed at 2940 cm^{-1} and 2989 cm^{-1} correspond to the C–H stretching vibrations commonly present in bioactive compounds. Furthermore, A broad band centered around 3363 cm^{-1} was assigned to O–H stretching vibrations, associated with hydroxyl-containing compounds, including moisture and bioactive compounds such as phenolic acids and flavonoids (Kalajahi and Ghandiha, 2022). The FTIR spectra of the encapsulated powders revealed characteristic absorption bands corresponding to polysaccharides, proteins, and the bioactive compounds. The spectra of the MD-based formulations showed strong C–O–C and C–O stretching vibrations between 1000 – 1200 cm^{-1}, which are typical of maltodextrin (Kalajahi and Ghandiha, 2022; Kang *et al.*, 2019). The combination of different encapsulation types (GA, MS, SPI, and WPI) causes changes in intensity in this region. A peak associated with carbonyl group of GA at 1597 cm^{-1} was observed in the spectra of encapsulated powder with MD-GA (Kang *et al.*, 2019). Peaks were also observed at approximately 1638 cm^{-1} and at 1449 cm^{-1} in the MD-SPI formulation, with higher intensity in the MD-WPI formulation. These correspond to amide I and amide II bands, respectively, characteristic of protein structure (Yao *et al.*, 2023), thus confirming the presence of soy protein and milk protein in the matrix. Following

microencapsulation, most of the encapsulated powders still showed the distinct O–H stretching vibrations characteristic of polyphenols at 3293, 3289, 3372, and 3306 cm^{-1}. However, the intensity of these peaks decreased compared to the extract. Similarly, the peaks at 2922, 2924, and 2926 cm^{-1} showed the presence of bioactive compounds retained in the encapsulated powder (George *et al.*, 2021). Overall, the FTIR results indicate effective incorporation of the extract into different coating matrices and suggest the presence of wall–core compatibility, with potential interactions influenced by the chemical nature of the wall materials.

(a)

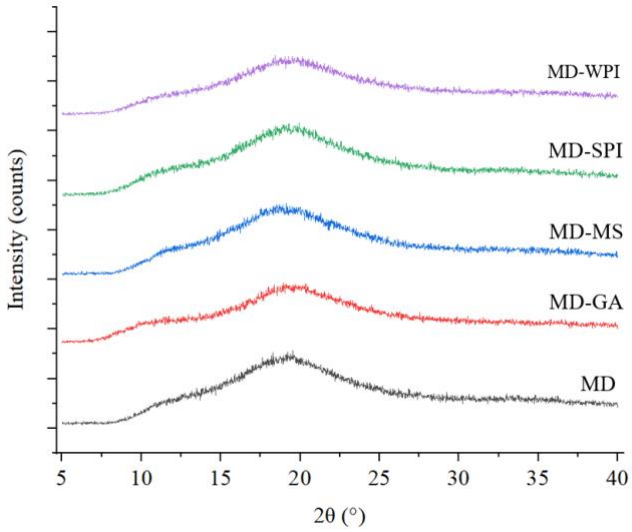

(b)

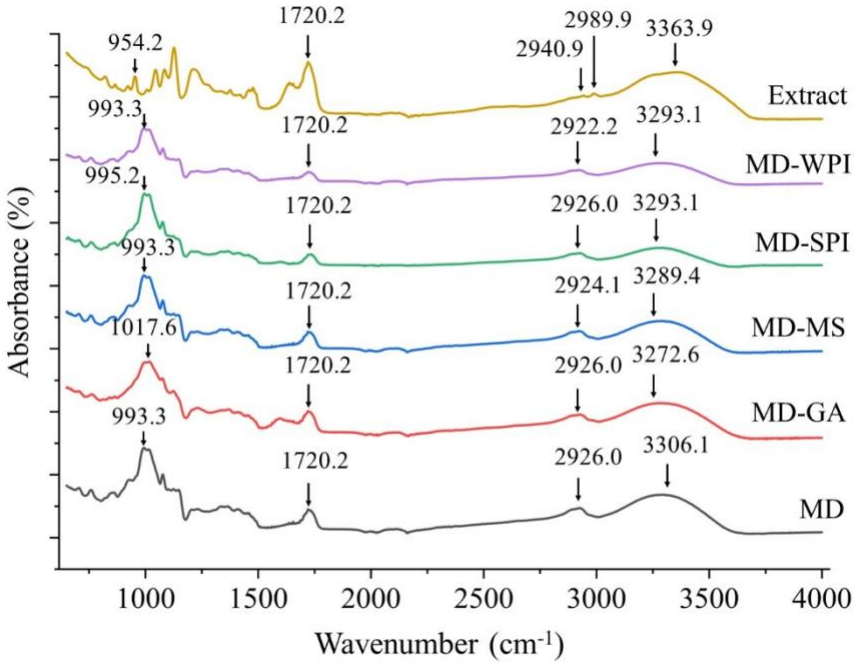

(c)

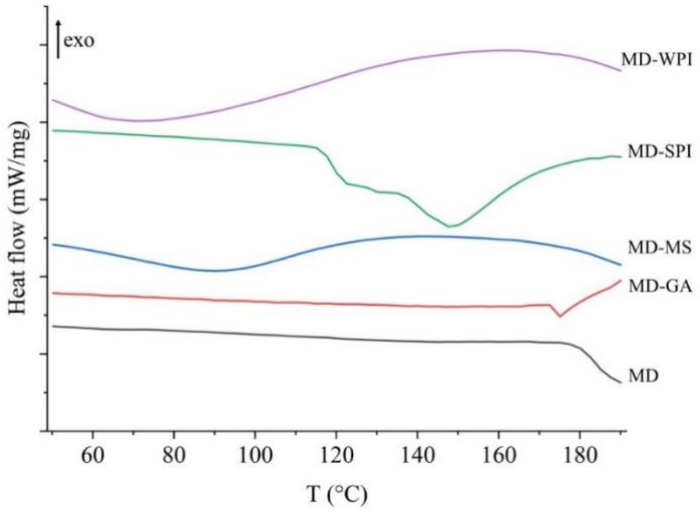

Figure 2. Effect of wall material type on (a) XRD, (b) FTIR, and (c) DSC profiles of the encapsulated powder

The DSC was conducted to evaluate the thermal behavior of the spray-dried microcapsules, as presented in Figure 2c. In the temperature range below 180 °C, the MD sample maintained a relatively flat heat flow curve, suggesting the absence of major thermal transitions within this range. This behavior indicates that maltodextrin alone forms a thermally stable matrix under tested thermal conditions. The incorporation of wall materials altered the DSC profiles of the encapsulated powders. The MD-GA formulation exhibited a slight deviation in heat flow around 175 °C, which may be attributed to the presence of low molecular weight fractions in GA that are more sensitive to thermal exposure. Despite this minor thermal event, the MD-GA powder maintained a comparatively stable thermal profile compared to the other wall material combinations. In contrast, microcapsules prepared using MD-MS, MD-SPI, and MD-WPI showed more pronounced and irregular heat flow patterns below 180 °C, indicating the presence of additional thermal transitions. Specifically, MD-MS and MD-WPI formulations displayed endothermal peaks in the temperature range of 70 – 180 °C (approximately 87 °C and 72 °C, respectively). The MD-SPI formulation exhibited an endothermic peak between 110 and 160 °C, likely related to thermal denaturation or structural transitions of soy protein. These findings suggest that while starch- or protein-based wall materials contribute to the encapsulation matrix, they introduce components that are more thermally labile. In contrast, MD and MD-GA formulations demonstrated better thermal resistance, making them more suitable for spray-drying conditions at temperatures below 180 °C.

SEM analysis was used to examine the surface morphology of spray-dried powders prepared with various wall materials, as illustrated in Figure 3. This analysis provided qualitative information on particle shape, porosity, surface smoothness, and particle integrity. All samples exhibited the characteristic spherical morphology typical of spray-dried microcapsules. However, the surface structure, apparent particle size, and aggregation behavior differed depending on the wall material used. For the powder formulated with MD alone, the particles were predominantly smooth and spherical, with minimal surface wrinkles. No evident particle agglomeration was observed. The MD-GA formulation also retained a spherical shape. The incorporation of GA, known for its water-retention capacity, led to localized surface deformation during rapid moisture removal, resulting in slight surface wrinkles. Despite this, the MD-GA particles exhibited no visible fractures, suggesting particle integrity. Particles from the MD-MS formulation were also

spherical and smooth. Additionally, the particles exhibited a tendency to aggregate, which may be related to increased surface stickiness or inter-particle adhesion during the drying process. In contrast, powders incorporating proteins (SPI and WPI) displayed irregular surface morphology with more pronounced wrinkling and roughness. These formulations included some particles that appeared deformed or fused, suggesting less uniform drying behavior and reduced morphological homogeneity compared to other wall material-based systems.

These findings underscore the significant impact of wall material composition on the morphology and overall quality of the spray-dried powders. Among the investigated formulations, the MD-GA combination demonstrated the most favorable characteristics, including spherical shape and intact surface morphology without visible fractures. When correlated with other analytical results such as the high microencapsulation efficiency, low water activity (below 0.2), and favorable thermal and physicochemical properties (as evidenced by XRD, FTIR, DSC, and SEM analyses), the MD-GA formulation emerges as the most effective system for encapsulating bioactive compounds from grape pomace extract under the spray-drying conditions in this study.

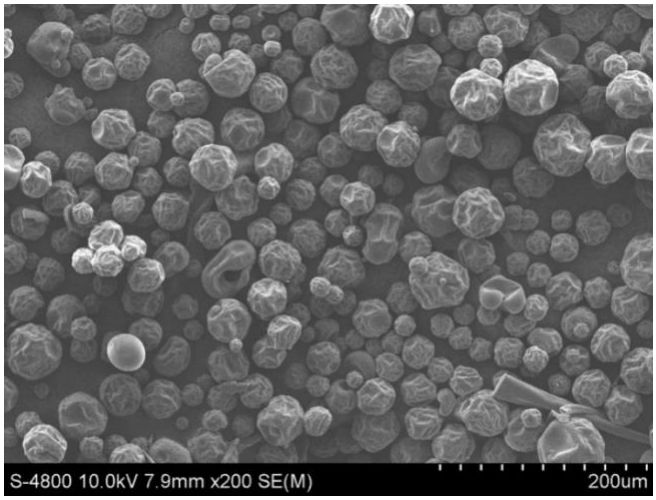

MD-GA

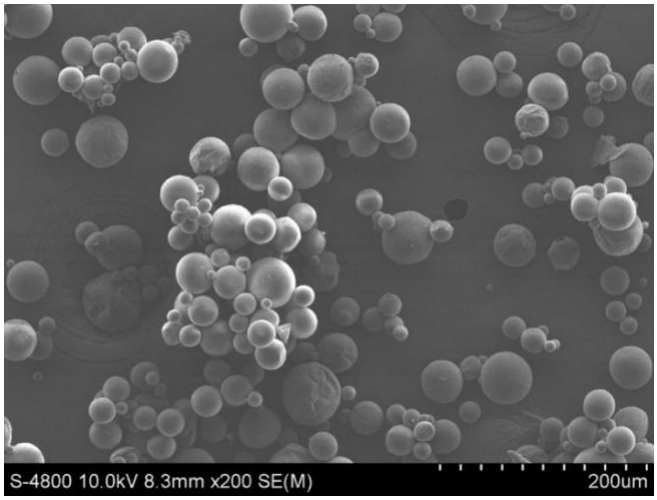

MD-MS

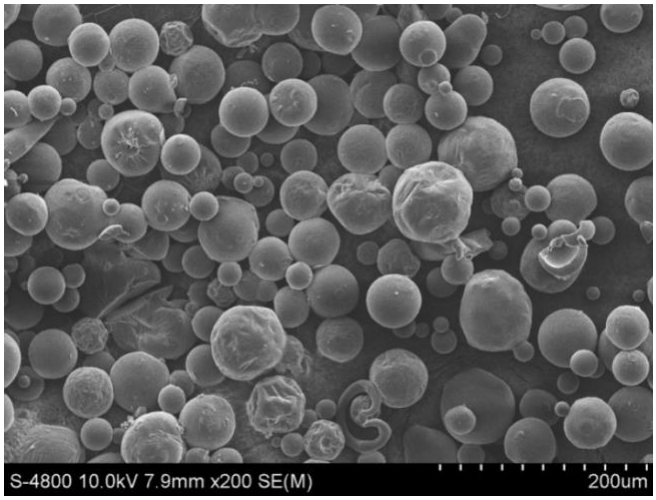

MD-SPI

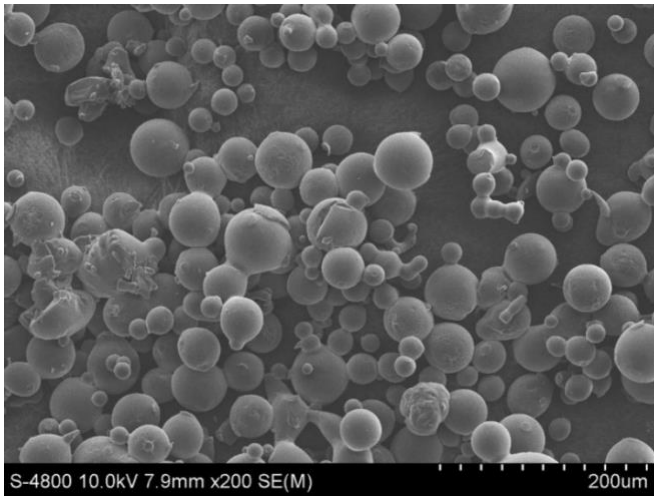

MD-WPI

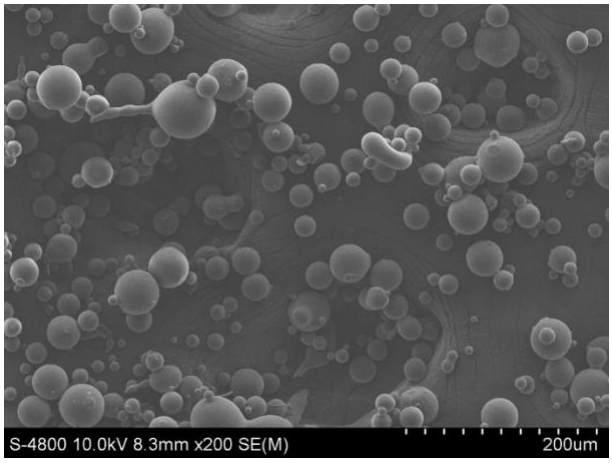

MD

Figure 3. Effects of wall material type on powder particle morphology at 200x magnification

3.2. Effects of core-to-wall material ratio on the encapsulation

The effect of the core-to-wall material ratio on encapsulation performance was evaluated using a fixed MD-GA ratio of 1:2 (w/w), a homogenization speed of 8,100 rpm for 10 min, an inlet air temperature of 170 °C, and a feed flow rate of 15 mL/min. As shown in Figure 1c, there are statistically significant differences among the ratios tested ($P \leq 0.05$). The highest encapsulation yield was achieved at a core-to-wall ratio of 1:4 (w/w), reaching 80.67 ± 2.09%, whereas the lowest value was observed at 1:6 (w/w). A core-to-wall ratio of 1:4 appears to offer a balanced composition, providing sufficient wall material to effectively encapsulate and protect the core compounds while maintaining high bioactive retention. A similar decreasing trend in retained phenolic content with increasing wall material proportion has been reported for grape polyphenols encapsulation using MD and GA (Tolun *et al.*, 2016). For TSC, there were no statistically significant differences in encapsulation yield across the tested different core-to-wall ratios ($P > 0.05$), with values ranging from 82.07% to 87.00%. This result may be related to the amphiphilic nature of saponins, which facilitates their dispersion and interaction with the MD-GA, leading to stable encapsulation across different ratios (Vincken *et al.*, 2007). In contrast, the encapsulation yield in terms of PAC was significantly influenced by the core-to-wall ratio ($P \leq 0.05$). The encapsulation yield of PAC decreased from 77.86 ± 1.84% at 1:3 (w/w) to 71.73 ± 0.35% at 1:6 (w/w). Proanthocyanidins are polyphenolic compounds rich in hydroxyl groups, which enable hydrogen bonding with wall materials such as MD and GA. This has been reported to stabilize the structure and minimize compound loss during spray drying, thereby improving encapsulation efficiency. However, at higher wall material concentrations, the reduced availability of core per unit mass of feed may limit effective interactions, leading to lower bioactive retention (Romano *et al.*, 2017). Furthermore, excessive use of wall material can negatively impact the overall bioactive content in the final powder, compromising its functional value. Therefore, based on results for TPC and TSC, a core-to-wall ratio of 1:4 (w/w) can be considered the most suitable ratio for maximizing encapsulation yield of bioactive compounds.

The influence of varying core-to-wall ratios (1:3, 1:4, 1:5, and 1:6, w/w) on encapsulation efficiency was investigated (Figure 1d). For TPC, the highest encapsulation efficiencies were observed at core-to-wall ratios of 1:4 and 1:5 (w/w), and no statistically significant difference was detected between these two ratios ($P > 0.05$). However, a further increase in the wall material (1:6, w/w) resulted in a slight but significant decrease in TPC encapsulation efficiency to 95.73 ± 0.42%. In the case of TSC, encapsulation efficiencies remained consistently

high at core-to-wall ratios of 1:4, 1:5, and 1:6 (w/w), with no statistically significant difference observed ($P > 0.05$). This stability may be attributed to the amphiphilic nature of saponins, as mentioned in the section on encapsulation yield. For PAC, the encapsulation efficiency ranged from 91.45% to 94.54%, with the highest value recorded at the 1:5 (w/w) ratio. The relatively high efficiency can be attributed to the ability of proanthocyanidins, rich in hydroxyl groups, to form hydrogen bonds with wall components. Increasing the wall material content improves encapsulation efficiency up to a favorable range (Fang and Bhandari, 2010). Beyond this threshold, excess wall material may hinder proper particle formation, leading to reduced encapsulation efficiency.

The results showed that increasing the core-to-wall material ratio led to a reduction in moisture content while water activity showed an increasing trend (Table 1). The core-to-wall ratios of 1:3 and 1:4 (w/w) did not show statistically significant differences in either moisture content or water activity ($P > 0.05$). Moisture content also showed significant variation, decreasing to 4.72 ± 1.06% at the highest ratio (1:6). The reduction in moisture content with increasing wall material proportion is consistent with previous studies reporting that increasing wall material concentrations reduced the moisture content of encapsulated powders during the encapsulation of red grape bioactives (Boonchu and Utama-Ang, 2015). Similarly, Tuyen *et al.* (2010) reported that the higher MD concentrations increased the solid content of the spray-drying feed, thus lowering the final product's moisture content. In contrast, the observed increase in water activity at higher core-to-wall material ratios may be attributed to a reduced proportion of DES extract in the formulation. DES extracts, known for their high viscosity and strong water retention, contribute to higher feed viscosity. Therefore, lowering their relative content may decrease the amount of bound water, leaving a larger fraction of free water in the final powder.

SEM micrographs (Figure 4) show clear morphological differences among powders prepared at the various core-to-wall material ratios. At a 1:3 (w/w) core-to-wall ratio, the particles exhibited irregular shapes with numerous surface indentations. The uneven surface and non-uniform particle sizes suggest insufficient wall material to form a continuous and mechanically robust encapsulating matrix. At a ratio of 1:4 (w/w), the powder displayed a spherical morphology with relatively smooth surfaces. For the 1:5 (w/w) ratio, the powder showed a wrinkled surface. While the particles were relatively spherical, the increased presence of wall material led to the formation of surface wrinkles, likely due to the rapid drying and shrinkage effects that occur during spray-drying with higher wall material content. At the highest ratio, 1:6 (w/w), particles exhibited significant structural deformation, with deep indentations and more pronounced wrinkling. These effects can be attributed to a reduced proportion of core, which diminishes the plasticizing effect of the core material. Additionally, enhanced shell rigidity combined with the sudden water evaporation during drying likely intensified particle collapse and surface shrinkage.

In conclusion, the 1:4 (w/w) core-to-wall ratio produced powders with the most favorable characteristics, including smooth and spherical particles and enhanced structural integrity. These advantages, combined with high encapsulation efficiency and suitable water activity, indicate that this ratio is the most appropriate choice for the encapsulation of grape pomace extract via spray drying under the investigated conditions.

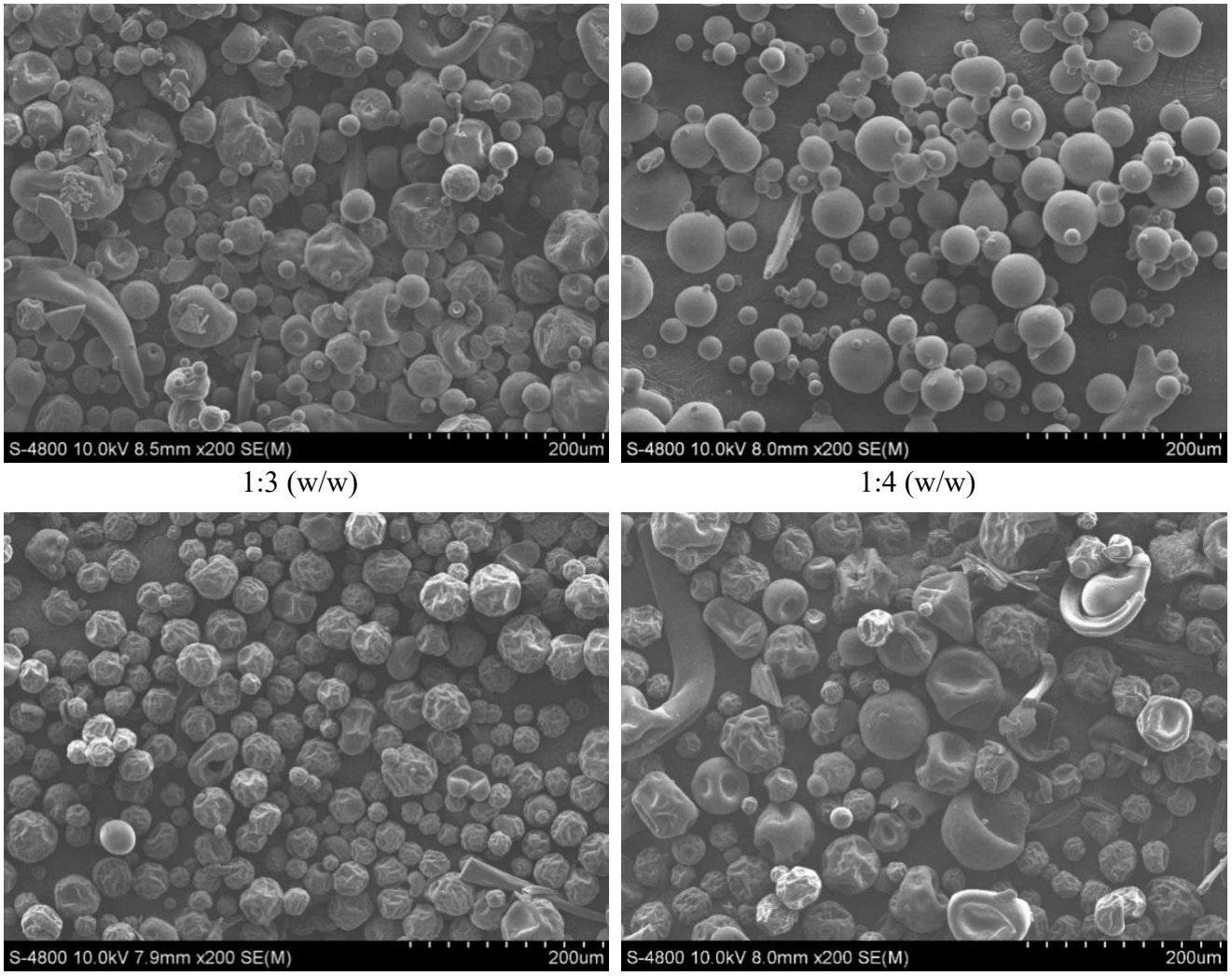

Figure 4. Effects of core-to-wall material ratio on powder particle morphology at 200x magnification

3.3. Effects of MD-to-GA ratio on the encapsulation

This experiment was conducted using a fixed core-to-wall ratio of 1:4 (w/w), a homogenization speed of 8,100 rpm for 10 min, an inlet air temperature of 170 °C, and a feed flow rate of 15 mL/min. The encapsulation yield and encapsulation efficiency of TPC, TSC, and PAC were assessed under different MD-to-GA ratios. Among the tested ratios, the MD-to-GA ratios of 2:1 and 3:1 (w/w) resulted in the highest encapsulation yield for all evaluated compounds (Figure 1e). For TSC, the 2:1 (w/w) ratio gave the highest yield at 88.00 ± 0.04%, although it was not statistically different from that at the 1:2 ratio ($P > 0.05$). Similarly, PAC encapsulation yield maximized at the 2:1 and 3:1 (w/w) ratio. These results are consistent with a previous finding showing that recovery yields decreased when the GA proportion exceeded optimal levels (Tolun *et al.*, 2016), likely due to increased feed viscosity and reduced atomization efficiency. The encapsulation efficiency for TPC was highest at the ratio of 1:1 (w/w), reaching 98.17 ± 0.02%, followed closely by the 2:1 (w/w) ratio (Figure 1f). For TSC, the highest efficiency was obtained at the 2:1 ratio. In the case of PAC, no statistically significant differences were found ($P > 0.05$). These results highlight the importance of balancing maltodextrin and gum arabic proportions in wall material composition.

Table 1 summarizes the moisture content and water activity of the encapsulated powders at various MD-to-GA ratios. Statistically significant differences were observed across treatments ($P \leq 0.05$). The MD-to-GA ratio of 1:2 (w/w) resulted in the highest moisture content (6.93 ± 0.03%) and water activity (0.215 ± 0.005), whereas the 3:1 (w/w) ratio exhibited the lowest values for both parameters. Increasing the proportion of MD led to a reduction in both moisture content and water activity. In contrast, increasing GA led to an increase in the moisture content of the powder. MD's linear molecular structure and lower hydroxyl group content limit its ability to bind water, resulting in lower moisture retention (Xiao *et al.*, 2022). GA's branched structure and high hydroxyl group content enhance water retention through hydrogen bonding, leading to higher moisture content (Mahdi *et al.*, 2020). Although GA is beneficial for improving retention of bioactive compounds, excessive GA can increase powder moisture, which may negatively affect storage stability. However, when the GA ratio is too low, as observed in the 3:1 (w/w) ratio, it results in affected powder morphology. Specifically, the powder becomes more prone to cracking, as confirmed by SEM images in Figure 5.

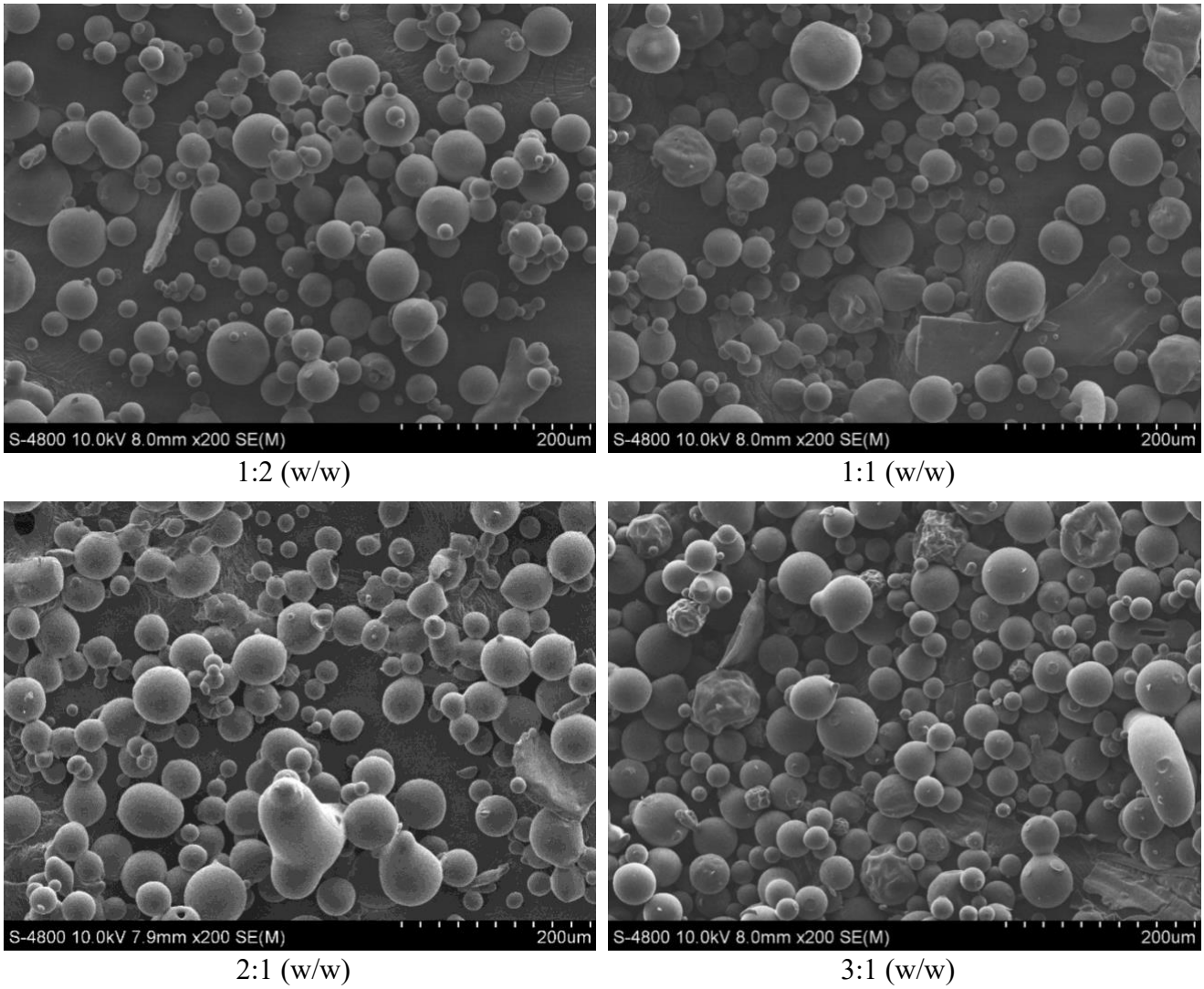

1:2 (w/w) 1:1 (w/w)

2:1 (w/w) 3:1 (w/w)

Figure 5. Effects of MD-to-GA ratio on powder particle morphology at 200x magnification

At the 1:1 (w/w) ratio, particles exhibited relatively uniform sizes at low magnification. However, higher magnification images revealed slight surface shrinkage, fine wrinkles, and small cracks. Some particles adhered together, suggesting that the GA content at this ratio may be insufficient to form a continuous coating layer around the core. Powders produced at the 1:2 (w/w) ratio had wrinkled surfaces with fewer cracks than those at the 1:1 (w/w) ratio. The 2:1 (w/w) ratio produced the most favorable morphology. Encapsulated particles were predominantly spherical with relatively smooth surfaces. Though some deformed particles were observed, the overall shape uniformity was maintained. In contrast, at the 3:1 (w/w) ratio, where MD content exceeded GA, the powders displayed pronounced wrinkling and structural deformation, likely due to insufficient GA to impart matrix flexibility.

Among the MD-to-GA ratios examined, the 2:1 (w/w) ratio provided the best balance between physicochemical and morphological characteristics. It achieved high encapsulation yield and efficiency, acceptable moisture content and water activity, and generated well-formed microcapsules with smooth surfaces and minimal deformation or cracking.

3.4. Effects of homogenization speed and duration on the encapsulation

The effects of homogenization speed and duration on encapsulation performance were investigated at fixed parameters, including an MD-to-GA ratio of 2:1 (w/w), core-to-wall ratio of 1:4 (w/w), inlet air temperature of 170 °C, and feed flow rate of 15 mL/min. The encapsulation yields for TPC, TSC, and PAC are presented in Table 2. In general, a homogenization speed of 10,800 rpm resulted in higher encapsulation yields than 8,100 rpm. At both speeds, increasing the homogenization duration from 5 to 10 min initially improved encapsulation yield. However, extending the duration to 15 min did not further enhance the yield and, in some cases, caused a slight reduction.

Table 2. Influence of homogenization speed and duration on the encapsulation yield, encapsulation efficiency and properties of the encapsulated powder

Speed (rpm)	Duration (min)	Encapsulation yield (%)		
		TPC	TSC	PAC
8,100	5	$61.52^{c} \pm 1.40$	$77.01^{c} \pm 2.60$	$80.22^{b} \pm 2.05$
	10	$84.61^{ab} \pm 0.43$	$86.25^{a} \pm 0.85$	$86.00^{ab} \pm 2.05$
	15	$83.34^{b} \pm 1.44$	$81.82^{b} \pm 0.76$	$87.60^{a} \pm 3.90$
10,800	5	$86.74^{a} \pm 0.43$	$82.31^{b} \pm 0.68$	$85.72^{ab} \pm 0.73$
	10	$87.10^{a} \pm 0.45$	$87.16^{a} \pm 1.37$	$88.50^{a} \pm 0.82$
	15	$84.84^{ab} \pm 0.97$	$84.74^{ab} \pm 1.12$	$85.31^{ab} \pm 2.25$
Speed (rpm)	**Duration (min)**	**Encapsulation efficiency (%)**		
		TPC	**TSC**	**PAC**
8,100	5	$96.51^{d} \pm 0.04$	$99.13^{bc} \pm 0.09$	$94.33^{b} \pm 0.04$
	10	$97.20^{b} \pm 0.10$	$99.34^{a} \pm 0.07$	$95.32^{a} \pm 0.09$
	15	$97.11^{b} \pm 0.02$	$99.02^{c} \pm 0.07$	$94.45^{b} \pm 0.08$
10,800	5	$96.93^{c} \pm 0.04$	$98.10^{e} \pm 0.06$	$92.95^{c} \pm 0.08$
	10	$97.91^{a} \pm 0.06$	$99.31^{ab} \pm 0.05$	$95.27^{a} \pm 0.14$
	15	$96.32^{e} \pm 0.02$	$98.56^{d} \pm 0.08$	$92.83^{c} \pm 0.13$
Speed (rpm)	**Duration (min)**	**Moisture content (%)**		**Water activity**
8,100	5	$4.47^{a} \pm 0.47$		$0.134^{a} \pm 0.008$
	10	$4.59^{a} \pm 0.32$		$0.141^{a} \pm 0.016$
	15	$4.22^{a} \pm 0.09$		$0.135^{a} \pm 0.023$
10,800	5	$3.78^{a} \pm 0.28$		$0.133^{a} \pm 0.010$
	10	$4.12^{a} \pm 0.24$		$0.135^{a} \pm 0.011$

	15	3.73[a] ± 0.44			0.137[a] ± 0.016		
Speed (rpm)	**Duration (min)**	**Mean (μm)**	**Mode (μm)**	**D_{10} (μm)**	**D_{50} (μm)**	**D_{90} (μm)**	**Span**
8,100	5	15.66	13.61	5.97	13.24	29.08	1.75
	10	15.57	12.40	5.94	13.01	28.83	1.76
	15	15.33	12.40	5.60	12.66	29.38	1.88
10,800	5	14.94	12.40	5.51	12.31	28.52	1.87
	10	14.37	12.40	5.20	12.08	26.84	1.79
	15	15.11	12.40	5.55	12.48	28.82	1.86

Distinct superscript letters within same parameter and column indicate statistically significant differences ($P \leq 0.05$).

At 8,100 rpm, increasing the duration from 5 to 10 min raised the TPC encapsulation yield, but a marginal decrease was observed at 15 min. In contrast, at 10,800 rpm, the encapsulation yields of TPC and PAC remained consistently high across all durations, with no significant differences between 5 and 10 min and only a slight decline at 15 min. Notably, the PAC encapsulation yields across treatments showed fewer significant variations, except at 8,100 rpm for 5 min, which recorded the lowest value (80.22%). These findings suggest that a homogenization speed of 10,800 rpm for 10 min is the most suitable condition for maximizing encapsulation yields of TPC, TSC, and PAC under the studied processing parameters. A low homogenization speed could lead to uneven droplet size distribution and incomplete coverage of the core material by the wall matrix, thereby reducing the coverage capability of the coating. Conversely, excessive homogenization speed or prolonged processing may induce excessive shear stress and localized heating, potentially destabilizing the suspension's stability. Short homogenization durations result in inadequate dispersion of the wall and extract phases, leading to an unstable suspension system and droplet aggregation during spray drying (Wang *et al.*, 2021).

Table 2 shows the effects of different homogenization speeds and durations on the encapsulation efficiency of TPC, TSC, and PAC. The highest encapsulation efficiency was determined at a homogenization speed of 10,800 rpm for 10 min, with values of 97.91% for TPC, 99.31% for TSC, and 95.27% for PAC. The next most effective condition was 8,100 rpm for 10 min. These findings suggest that 10 min is a sufficient duration to homogenize the particles evenly, long enough to ensure uniform dispersion without causing self-heating and promoting aggregation, both of which could reduce encapsulation efficiency (Kelly and Fox, 2016).

Moisture content and water activity did not differ statistically among the tested homogenization conditions ($P > 0.05$) (Table 2). The moisture content for all samples remained below 5%, while water activity values were below 0.20, indicating good stability and suitability for spray-dried powders. The absence of significant differences is consistent with previous studies reporting that variations in homogenization speed and duration have minimal effects on moisture content and water activity (Koç *et al.*, 2011). Likewise, another study has shown that while homogenization conditions strongly influence droplet size distribution and encapsulation stability, their impact on moisture content and water activity is comparatively limited (Alcântara *et al.*, 2019).

Table 2 shows that particle size parameters varied significantly with homogenization speed and duration ($P \leq 0.05$). Increasing the homogenization speed from 8,100 to 10,800 rpm resulted in a notable reduction in both mean particle size and size distribution. At 8,100 rpm, increasing the homogenization duration from 5 to 10 min led to a decrease in the average particle size, indicating improved dispersion efficiency. At a homogenization duration of 5 min, the mean particle sizes were the largest, indicating

poor dispersion and low uniformity. However, extending the homogenization duration further to 15 min resulted in increased D90 and span values, suggesting a broader particle size distribution, likely due to over-homogenization.

At 10,800 rpm, superior homogenization performance was observed, with all particle size parameters being smaller than those obtained at 8,100 rpm. Increasing the homogenization duration to 10 min produced smaller particles, with mean, D90, and span values of 14.37 μm, 26.84 μm, and 1.79, respectively, indicating highly efficient homogenization. A further increase to 15 min slightly increased the mean particle size to 15.11 μm, suggesting that excessive homogenization may cause re-agglomeration due to insufficient wall material to stabilize the increased surface area. These results are consistent with previous studies reporting optimal particle formation and powder stability at homogenization speeds of approximately 10,000 rpm for 10 min in encapsulation (Machamasi *et al.*, 2024). Similarly, spray-dried virgin coconut oil with homogenization speeds between 10,000 and 12,000 rpm for 10 min produced light-colored powders with excellent dispersion and narrow particle distributions (Nor *et al.*, 2021).

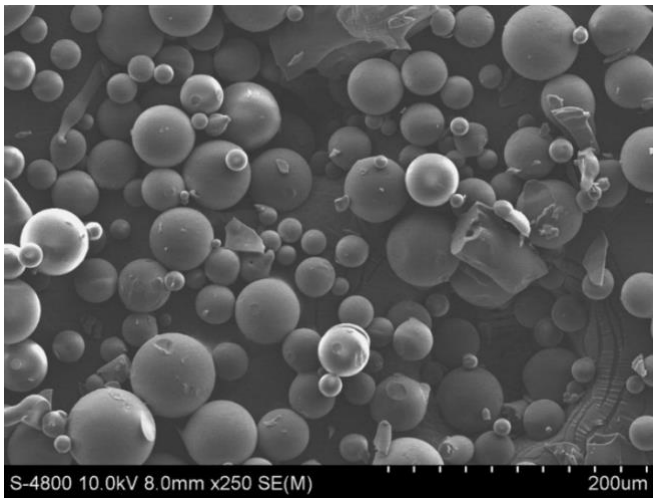

8,100 rpm – 5 min

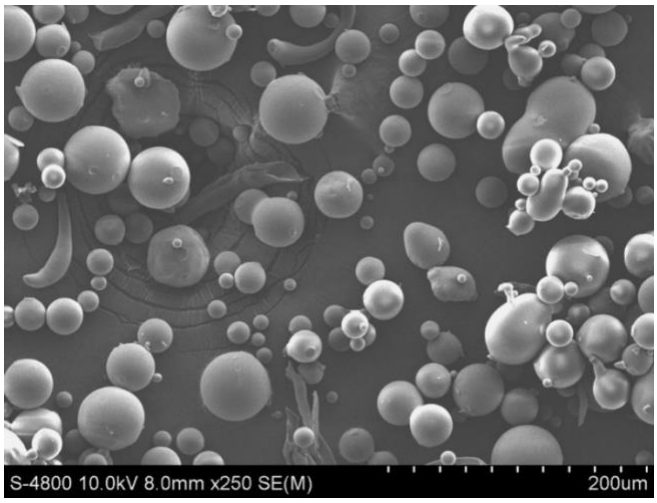

10,800 rpm – 5 min

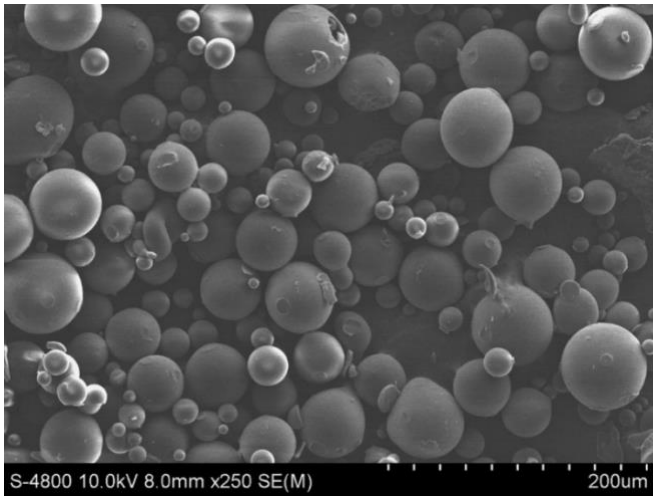

8,100 rpm – 10 min

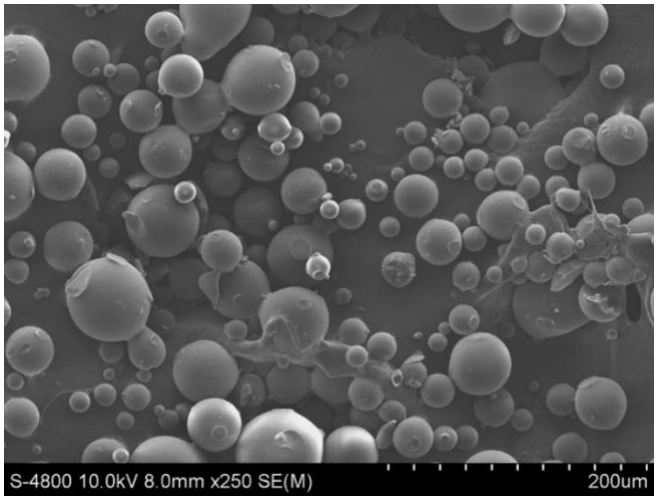

10,800 rpm – 10 min

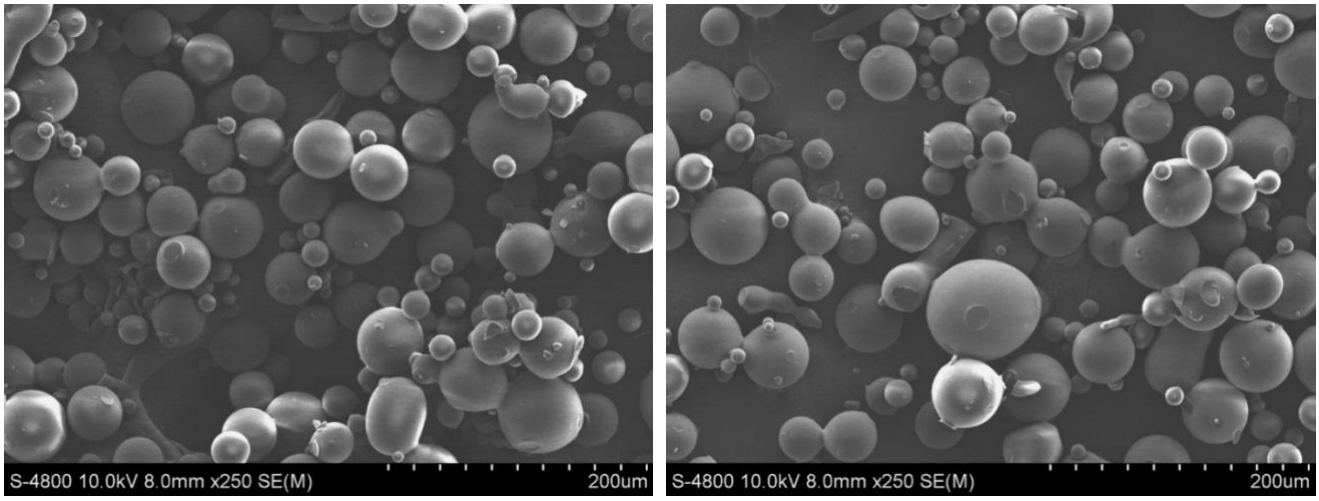

8,100 rpm – 15 min 10,800 rpm – 15 min

Figure 6. Effects of homogenization speed and duration on powder particle morphology at 250x magnification

SEM observations indicated that, across all homogenization regimes investigated, the spray-dried powders predominantly exhibited spherical particles with relatively smooth surfaces, and no obvious surface cracks were observed (Figure 6). Under the magnification conditions applied, clear morphological differences among powders at the various homogenization speeds and durations were not readily discernible. These observations suggest that, within the resolution of SEM, variations in homogenization parameters did not markedly influence the external surface morphology of powders produced using maltodextrin and gum arabic as wall materials.

In summary, while changes in homogenization speed and duration did not significantly affect moisture content, water activity, and morphology, they clearly impacted encapsulation efficiency and particle size distribution. Homogenization at 10,800 rpm for 10 min achieved a suitable balance between particle size reduction and suspension stability.

3.5. Effects of inlet air temperature on the encapsulation

The effects of inlet air temperature on encapsulation performance were evaluated while maintaining constant processing parameters, including an MD-GA ratio of 2:1 (w/w), core-to-wall ratio of 1:4 (w/w), homogenization speed at 10,800 rpm for 10 min, and feed flow rate of 15 mL/min. As shown in Figure 1g, the encapsulation yields significantly increased as the inlet air temperature rose from 140 °C to 160 – 170 °C, and decreased when the temperature reached 180 °C. The highest encapsulation yield was obtained at 160 °C. The improvement in encapsulation yield at 160 – 170 °C can be attributed to the enhanced evaporation rates, which facilitated rapid film formation around the bioactive compounds. This rapid evaporation minimizes prolonged exposure of the droplets to oxygen and moisture, thereby reducing oxidative losses. Conversely, at lower temperatures (140 and 150 °C), slower moisture removal delays film formation, increasing the susceptibility of bioactives to oxidation and interfacial degradation, which may result in reduced encapsulation yield. When the inlet air temperature reached 180 °C, thermal degradation of heat-sensitive compounds such as polyphenols and anthocyanins likely occurred, along with possible partial degradation of the wall material (Ruprecht *et al.*, 2022).

Encapsulation efficiency exhibited a similar trend (Figure 1h). The encapsulation efficiency for TPC increased to 98.73 ± 0.04% at 160 °C, followed by a slight decrease at 180 °C. The same pattern was observed for TSC and PAC, with the highest efficiencies at 160 °C.

However, PAC encapsulation efficiency remained relatively stable at 170 °C, with no statistically significant difference compared to 160 °C ($P > 0.05$). At optimal inlet air temperatures (160 and 170 °C), rapid evaporation promoted the formation of a uniform and stable coating, effectively encapsulating and protecting bioactive compounds. Conversely, excessively high inlet air temperatures (180 °C) may disrupt the balance between drying rate and film formation, potentially causing cracks, incomplete encapsulation, or thermal degradation of core (Noshad *et al.*, 2015). Based on these results, an inlet air temperature of 160 °C was identified as the most favorable condition for achieving high encapsulation yield and efficiency.

The moisture content of the powder decreased progressively with increasing the inlet air temperature, from 4.86 ± 0.12% at 140 ºC to 3.75 ± 0.11% at 180 ºC (Table 1). Moisture contents in the range of approximately 3 – 5% are generally considered acceptable for spray-dried powders. Maintaining a final moisture content below 5% is particularly important, as low moisture levels reduce the risk of sticking, caking, and undesirable oxidation reactions (Gharsallaoui *et al.*, 2007). Consequently, this improves the storage stability, flowability, and overall qualities of the powder. Moreover, reduced moisture content indirectly contributes to improved microbial stability and extended shelf life of the encapsulated powder. Despite the variation in moisture content, water activity values remained consistently low across all samples, with no statistically significant differences ($P > 0.05$), and all values were below 0.2. During the spray-drying, the solution droplets containing bioactive compounds and wall materials are atomized into fine particles and subjected to a stream of hot air. The initial exposure to high temperatures rapidly evaporates surface moisture, leading to the formation of a dry outer shell. This shell encapsulates the remaining internal moisture in a bound form, thereby minimizing its influence on water activity (Gharsallaoui *et al.*, 2007).

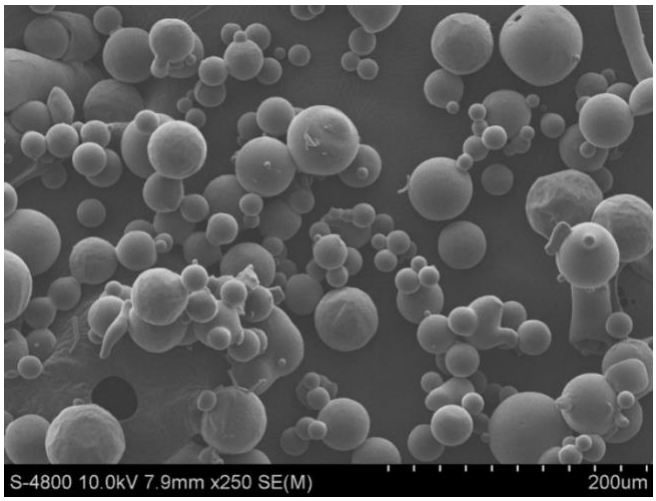

140 °C

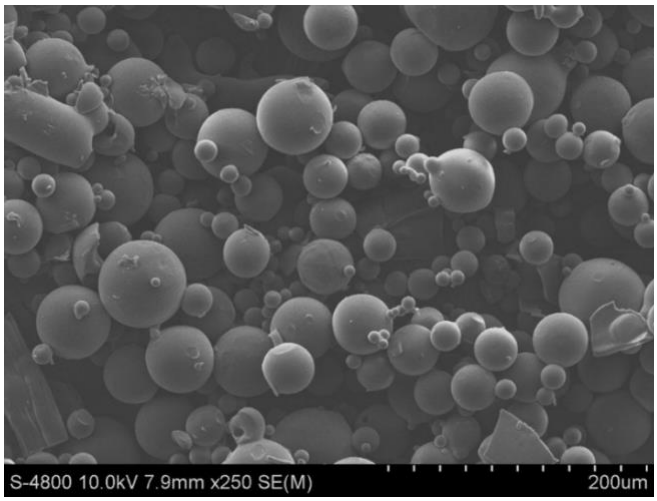

150 °C

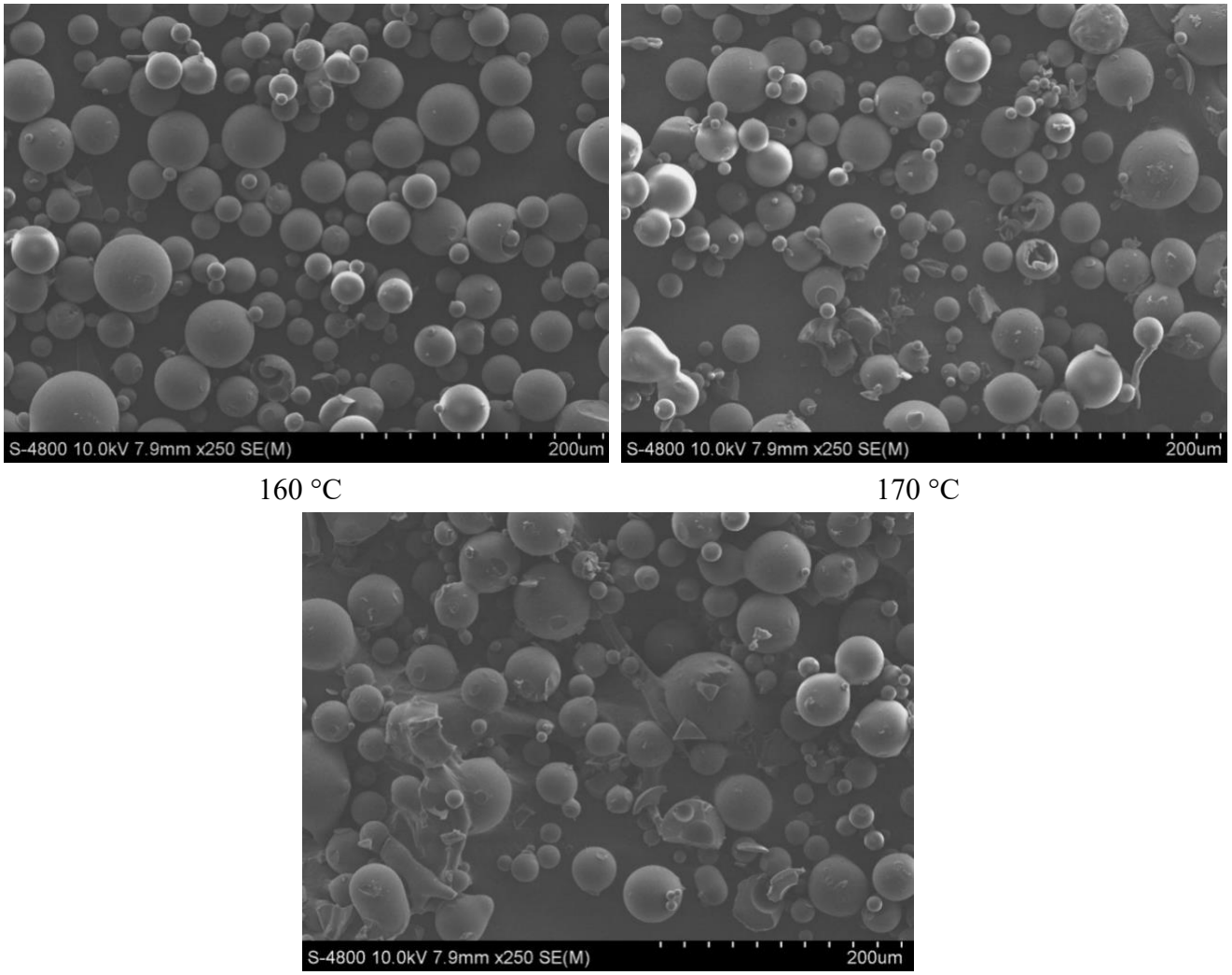

160 °C 170 °C

180 °C

Figure 7. Effects of inlet air temperature on powder particle morphology at 250x magnification

SEM analysis revealed that powders produced at all inlet air temperatures exhibited generally smooth, spherical particles with minimal deformation or surface wrinkles (Figure 7). This morphology was attributed to the use of a wall material composed of MD and GA. Powders obtained at 150 °C showed greater variability in particle size and shape compared to those produced at 160 °C. Insufficient drying temperatures led to non-uniform moisture removal, resulting in structural inconsistency (Pajareon and Theerakulkait, 2017). At lower temperatures, uneven evaporation can cause some particles to retain excess water, producing larger particles, while others dry more rapidly and shrink, contributing to variability in size and morphology. At higher inlet air temperatures (170 or 180 °C), increased surface deformation was observed, including cracks and fragmentation. Such defects may be associated with an imbalance between rapid water evaporation and proper film formation, which compromises wall integrity during drying (Noshad *et al.*, 2015). In contrast, microcapsules produced at 160 °C demonstrated the most uniform morphology, characterized by consistent spherical shape and minimal surface deformation.

Overall, the results of the SEM analysis, combined with encapsulation yield and efficiency, moisture content, and water activity, indicate that an inlet air temperature of 160 °C is the most appropriate for spray-drying grape

pomace extract using an MD-GA encapsulation system.

3.6. Effects of feed flow rate on the encapsulation

The effect of feed flow rate on the encapsulation of grape pomace extract was evaluated while keeping other parameters constant, including an MD-GA ratio of 2:1 (w/w), core-to-wall ratio of 1:4 (w/w), homogenization at 10,800 rpm for 10 min, and an inlet air temperature of 160 °C. As shown in Figure 1i, increasing the feed flow rate from 15 to 35 mL/min did not result in statistically significant differences in the encapsulation yields of TPC, TSC, and PAC. Within this range, encapsulation yields remained consistently high, above 85% for TPC and 80% for PAC. However, a pronounced decline in encapsulation yield was observed when the feed flow rate increased to 40 mL/min and 45 mL/min. Excessively high feed flow rates may exceed the heat and mass transfer capacity of the drying chamber, leading to greater material loss and lower drying efficiency (Ton and Dao, 2006). Moreover, higher feed rates likely reduce the effective residence time of droplets and promote non-uniform atomization, which negatively affects the encapsulation process (Gharsallaoui *et al.*, 2007).

Encapsulation efficiency results revealed statistically significant differences across feed flow rates ($P \leq 0.05$) (Figure 1j). While PAC encapsulation efficiency remained relatively stable at approximately 93%, slight declines were observed for TSC and TPC at higher feed flow rates. Shortened drying times at elevated feed rates may restrict solvent evaporation and hinder the development of a dense and continuous wall matrix, resulting in partial exposure of the bioactive compounds on the particle surface and reduced encapsulation efficiency. Overall, the results suggest that a feed flow rate in the range 15 – 35 mL/min was suitable for maintaining both high encapsulation yield and efficiency. Beyond this range, drying performance diminishes, compromising powder quality.

The feed flow rate significantly affected the moisture content of the spray-dried powders ($P \leq 0.05$), whereas no significant differences were observed in water activity ($P > 0.05$) (Table 1). Moisture content increased progressively as the feed flow rate rose from 15 mL/min to 45 mL/min. This trend can be attributed to the reduced residence time of droplets in the drying chamber at higher flow rates, which limits complete evaporation. In addition, higher feed flow rates introduce larger volumes of liquid into the chamber over a shorter period, thereby reducing the system's ability to fully remove moisture. Interestingly, water activity values remained relatively stable and below 0.20 across all treatments ($P > 0.05$). This phenomenon may be partly attributed to the presence of GA in the wall material. GA is known for its ability to retain water predominantly in a bound form due to its highly branched polysaccharide structure. This likely contributed to the retention of water within the particle matrix rather than as free water, thereby stabilizing water activity despite the increasing overall moisture content.

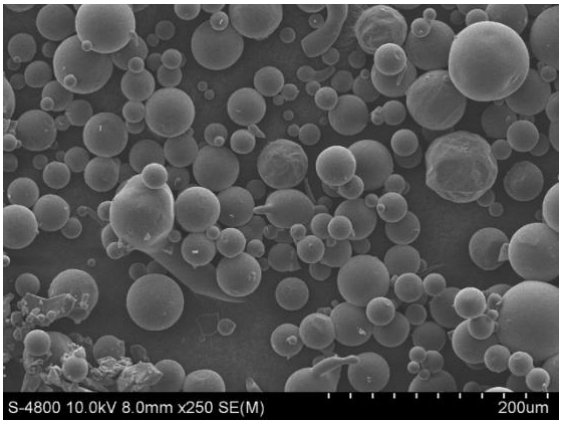

15 mL/min

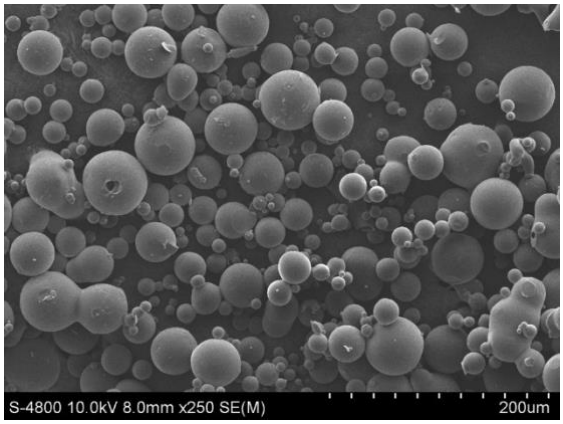

20 mL/min

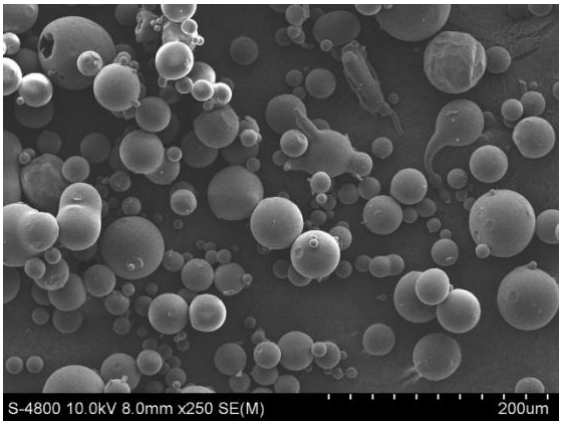

25 mL/min

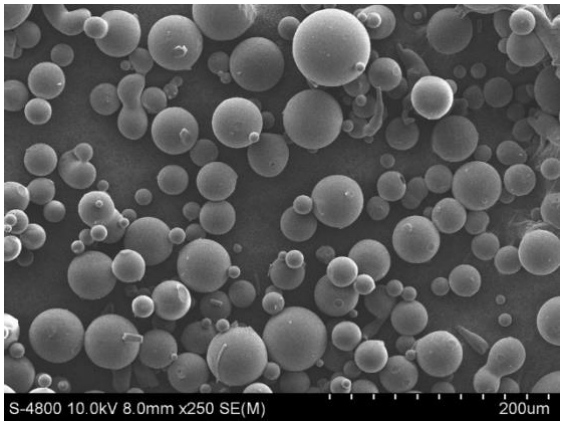

30 mL/min

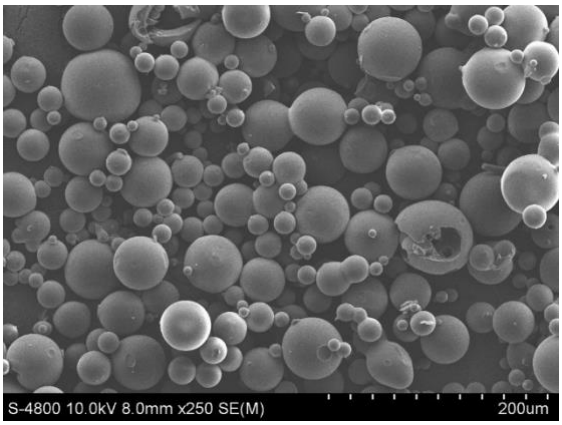

35 mL/min

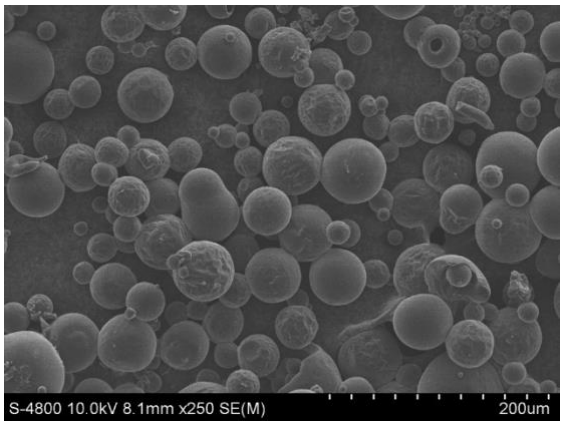

40 mL/min

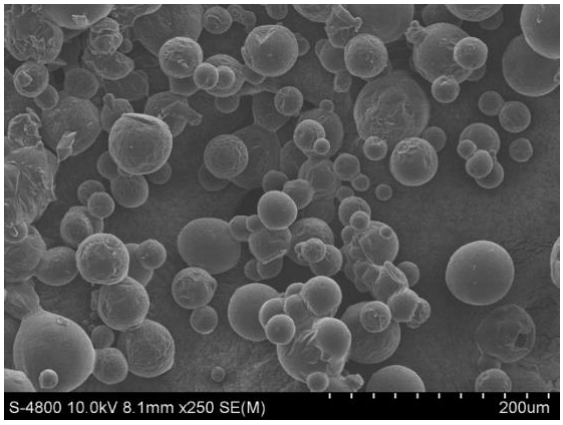

45 mL/min

Figure 8. Effects of feed flow rate on powder particle morphology at 250x magnification

The surface morphology of the microcapsules at various feed flow rates is shown in Figure 8 and Figure 9. Powder produced at feed flow rates between 15 and 35 mL/min exhibited uniform, spherical, and largely undeformed particles with smooth surfaces. These characteristics suggest stable spray-drying conditions, with adequate drying and wall formation. In contrast, increasing feed flow rates to 40 and 45 mL/min, distinct morphological changes were observed. Surface wrinkling and partial deformation began to appear at 40 mL/min, although particles did not exhibit visible cracking. At 45 mL/min, deformation became more prominent, with increased incidence of wrinkles, particle agglomeration, and irregular shapes. This deformation is attributed to reduced heat exchange efficiency, insufficient drying time, and the overaccumulation of atomized material

in the drying chamber. Moreover, elevated feed flow rates increase droplet size, making it more difficult for the heat to penetrate and dry the particles uniformly. Larger particles are more prone to collapsing and surface deformation (Ton and Dao, 2006).

Overall, a feed flow rate in the range of 15 – 35 mL/min was identified as suitable for spray drying under the tested conditions, producing powders with desirable moisture levels, stable water activity, and well-defined morphology. Among these conditions, the feed flow rate of 35 mL/min is recommended as the most practical choice for balancing product quality and process efficiency, particularly when considering scalability and drying time constraints at industrial levels.

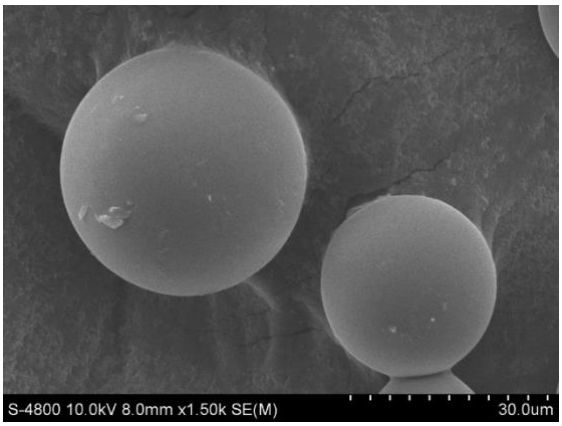

15 mL/min

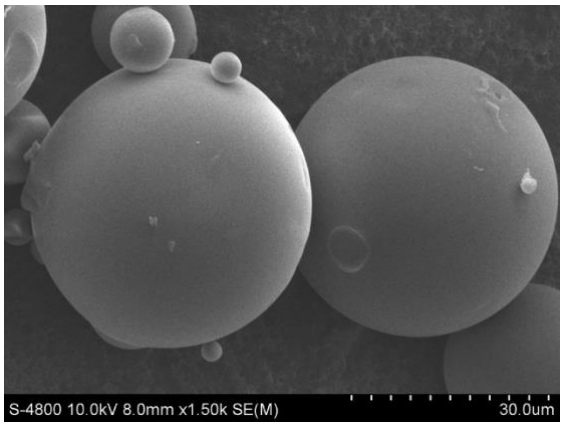

20 mL/min

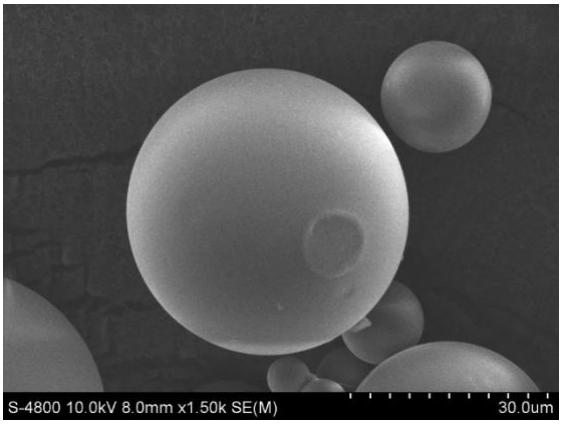

25 mL/min

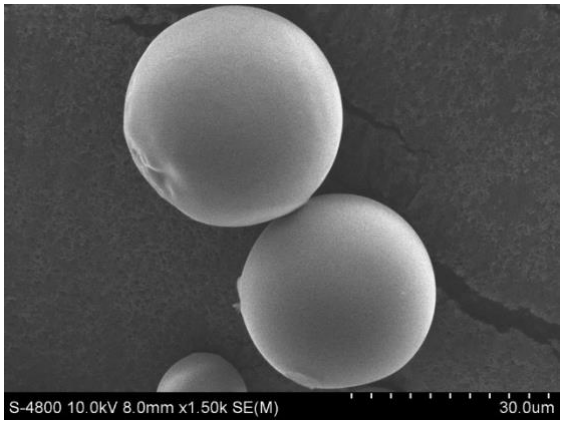

30 mL/min

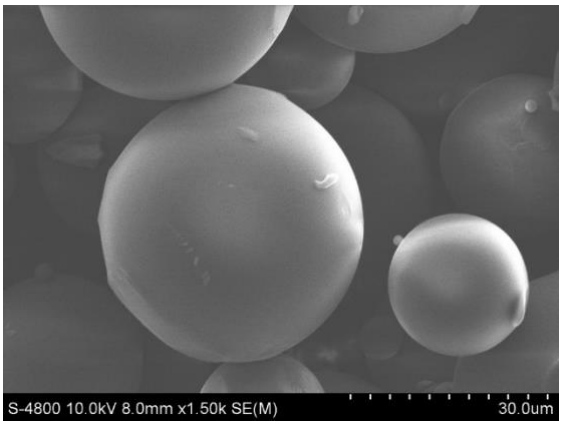

35 mL/min

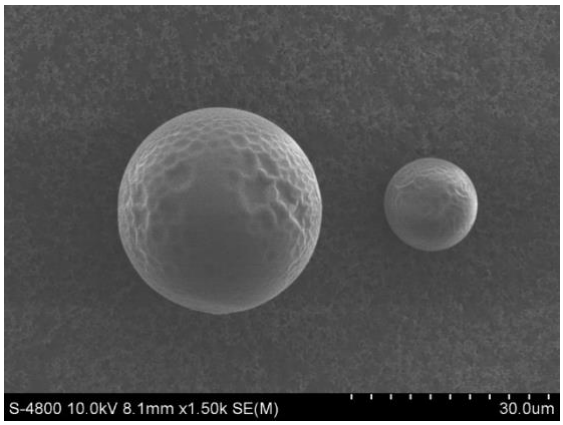

40 mL/min

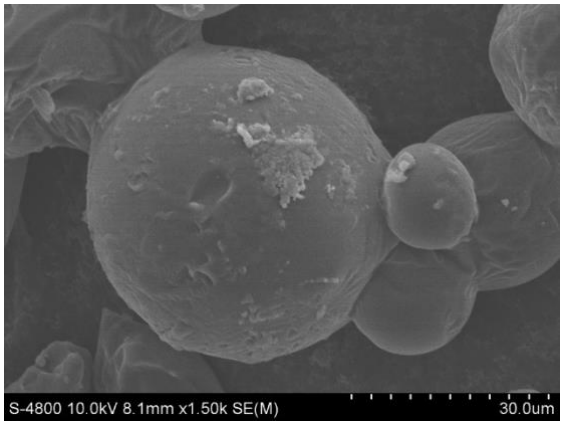

45 mL/min

Figure 9. Effects of feed flow rate on powder particle morphology at 1500x magnification

4. Conclusions

This research demonstrated the effective encapsulation of bioactive compounds extracted with DES from *Red Cardinal* grape pomace using spray-drying technology. Various key parameters, including wall material type, core-to-wall material ratio, MD-to-GA ratio, homogenization conditions, inlet air temperature, and feed flow rate, were systematically investigated for their influence on encapsulation yield, encapsulation efficiency, and physicochemical properties of the resulting powders. The most suitable encapsulation conditions were identified as an MD-to-GA ratio of 2:1 (w/w), a core-to-wall material ratio of 1:4 (w/w), homogenization at 10,800 rpm for 10 min, an inlet air temperature of 160 °C, and a feed flow rate of 35 mL/min. Under these conditions, the resulting microcapsules exhibited high encapsulation yields and efficiencies for TPC, TSC, and PAC, along with desirable moisture content and stable water activity. Characterization techniques including XRD, FTIR, DSC, and SEM confirmed the successful formation of microcapsules with uniform morphology and predominantly amorphous structure, indicating effective encapsulation and enhanced thermal stability of the bioactive compounds. These findings highlight the potential of DES as an environmentally friendly extraction solvent and spray-drying as a scalable encapsulation method to improve the stability and functionality of grape pomace bioactives. The resulting encapsulated powders offer promising applications in the food and pharmaceutical industries, contributing to the sustainable utilization of agro-industrial by-products.

5. References

Alcântara, M. A., de Lima, A. E. A., Braga, A. L. M., Tonon, R. V., Galdeano, M. C., da Costa Mattos, M., Santa Brígida, A. I., Rosenhaim, R., dos Santos, N. A., and de Magalhães Cordeiro, A. M. T. (2019). Influence of the emulsion homogenization method on the stability of chia oil microencapsulated by spray drying. *Powder Technology,* 354, 877-885. doi:https://doi.org/10.1016/j.powtec.2019.06.026

Boonchu, T., and Utama-Ang, N. (2015). Optimization of extraction and microencapsulation of bioactive compounds from red grape (*Vitis vinifera* L.) pomace. *Journal of Food Science and Technology,* 52, 783-792. doi:https://doi.org/10.1007/s13197-013-1079-7

Cano-Higuita, D. M., Vélez, H. A. V., and Telis, V. R. N. (2015). Microencapsulation of turmeric oleoresin in binary and ternary blends of gum Arabic, maltodextrin and modified starch. *Ciência e Agrotecnologia,* 39(2), 173-182. doi:https://doi.org/10.1590/S1413-70542015000200009

Dai, Y., Spronsen, J. V., Witkamp, G.-J., Verpoorte, R., and Choi, Y. H. (2013). Natural deep eutectic solvents as new

potential media for green technology. *Analytica Chimica Acta,* 766, 61-68. doi:http://dx.doi.org/10.1016/j.aca.2012.12.019

Fang, Z., and Bhandari, B. (2010). Encapsulation of polyphenols–a review. *Trends in Food Science & Technology,* 21(10), 510-523. doi:https://doi.org/10.1016/j.tifs.2010.08.003

Frank, D., Schenck, L., Koynov, A., Su, Y., Li, Y., and Variankaval, N. (2021). Optimizing solvent selection and processing conditions to generate high bulk-density, co-precipitated amorphous dispersions of posaconazole. *Pharmaceutics,* 13(12), 2017. doi:https://doi.org/10.3390/pharmaceutics13122017

George, T. T., Oyenihi, A. B., Rautenbach, F., and Obilana, A. O. (2021). Characterization of *Moringa oleifera* leaf powder extract encapsulated in maltodextrin and/or gum arabic coatings. *Foods,* 10(12), 3044. doi:https://doi.org/10.3390/foods10123044

Gharsallaoui, A., Roudaut, G., Chambin, O., Voilley, A., and Saurel, R. (2007). Applications of spray-drying in microencapsulation of food ingredients: An overview. *Food Research International,* 40(9), 1107-1121. doi:https://doi.org/10.1016/j.foodres.2007.07.004

Jafari, S., Jafari, S. M., Ebrahimi, M., Kijpatanasilp, I., and Assatarakul, K. (2023). A decade overview and prospect of spray drying encapsulation of bioactives from fruit products: Characterization, food application and in vitro gastrointestinal digestion. *Food Hydrocolloids,* 134, 108068. doi:https://doi.org/10.1016/j.foodhyd.2022.108068

Janiszewska-Turak, E., Walczak, M., Rybak, K., Pobiega, K., Gniewosz, M., Woźniak, Ł., and Witrowa-Rajchert, D. (2022). Influence of fermentation beetroot juice process on the physico-chemical properties of spray dried powder. *Molecules,* 27(3), 1008. doi:https://doi.org/10.3390/molecules27031008

Kalajahi, S. E. M., and Ghandiha, S. (2022). Optimization of spray drying parameters for encapsulation of Nettle (*Urtica dioica* L.) extract. *LWT,* 158, 113149. doi:https://doi.org/10.1016/j.lwt.2022.113149

Kang, Y.-R., Lee, Y.-K., Kim, Y. J., and Chang, Y. H. (2019). Characterization and storage stability of chlorophylls microencapsulated in different combination of gum Arabic and maltodextrin. *Food Chemistry,* 272, 337-346. doi:https://doi.org/10.1016/j.foodchem.2018.08.063

Kelly, A. L., and Fox, P. F. (2016). Manufacture and properties of dairy powders. In Paul L. H. McSweeney & J. A. O'Mahony (Eds.), *Advanced Dairy Chemistry: Volume 1B: Proteins: Applied Aspects* (pp. 1-33). Ireland: Springer Science+Business Media.

Koç, M., Koç, B., Susyal, G., Sakin Yilmazer, M., Kaymak Ertekin, F., and Bağdatlıoğlu, N. (2011). Functional and physicochemical properties of whole egg powder: effect of spray drying conditions. *Journal of Food Science and Technology,* 48, 141-149. doi:https://doi.org/10.1007/s13197-010-0159-1

Li, Y., Guo, C., Yang, J., Wei, J., Xu, J., and Cheng, S. (2006). Evaluation of antioxidant properties of pomegranate peel extract in comparison with pomegranate pulp extract. *Food Chemistry,* 96(2), 254-260. doi:https://doi.org/10.1016/j.foodchem.2005.02.033

López-Astorga, M., Leon-Bejarano, M., Gámez-Meza, N., Del Toro-Sánchez, C. L., Simsek, S., and Ovando-Martínez, M. (2025). Microencapsulated grape pomace extract as an antioxidant ingredient added to Greek-style yogurt: Storage stability an in vitro bioaccessibility. *Food Chemistry,* 477, 143550. doi:https://doi.org/10.1016/j.foodchem.2025.143550

Machamasi, R., Hwang, S.-J., and Dinh, L. (2024). The Formulation, Preparation, and Evaluation of Celecoxib Nanosuspensions: Nanosizing via High-Pressure

Homogenization and Conversion of the Nanosuspensions into Dry Powders by Spray Drying and Freeze Drying. *Journal of Pharmaceutical and BioTech Industry,* 1(1), 20-37. doi:https://doi.org/10.3390/jpbi1010004

Mahdi, A. A., Mohammed, J. K., Al-Ansi, W., Ghaleb, A. D., Al-Maqtari, Q. A., Ma, M., Ahmed, M. I., and Wang, H. (2020). Microencapsulation of fingered citron extract with gum arabic, modified starch, whey protein, and maltodextrin using spray drying. *International Journal of Biological Macromolecules,* 152, 1125-1134. doi:https://doi.org/10.1016/j.ijbiomac.2019.10.201

Mariod, A. A. (2018). Chemical properties of gum Arabic. In A. A. Mariod (Ed.), *Gum arabic: Structure, Properties, Application and Economics* (pp. 67-73). Sudan: Elsevier.

Moreno, T., De Paz, E., Navarro, I., Rodríguez-Rojo, S., Matías, A., Duarte, C., Sanz-Buenhombre, M., and Cocero, M. (2016). Spray drying formulation of polyphenols-rich grape marc extract: Evaluation of operating conditions and different natural carriers. *Food and Bioprocess Technology,* 9, 2046-2058. doi:https://doi.org/10.1007/s11947-016-1792-0

Negrao-Murakami, A. N., Nunes, G. L., Pinto, S. S., Murakami, F. S., Amante, E. R., Petrus, J. C. C., Prudêncio, E. S., and Amboni, R. (2016). Influence of DE-value of maltodextrin on the physicochemical properties, antioxidant activity, and storage stability of spray dried concentrated mate (Ilex paraguariensis A. St. Hil.). *LWT Food Science and Technology,* 79, 1-7. doi:https://doi.org/10.1016/j.lwt.2016.11.002

Nor, N. F. A., Ya'akob, H., Ngadiran, S., Idris, A., Anuar, N. S., and Sarmidi, M. R. (2021). Evolutions in virgin coconut oil: Liquid to powder. *Jurnal Teknologi (Sciences & Engineering),* 83(3), 119-132. doi:https://doi.org/10.11113/jurnalteknologi.v83.16265

Noshad, M., Mohebbi, M., Koocheki, A., and Shahidi, F. (2015). Microencapsulation of vanillin by spray drying using soy protein isolate–maltodextrin as wall material. *Flavour and Fragrance Journal,* 30(5), 387-391. doi:https://doi.org/10.1002/ffj.3253

Nguyen, D. Q., Mounir, S., and Allaf, K. (2017). Optimization of the spray drying operating conditions for producing the powder mixture of gum Arabic and maltodextrin. *International Journal of Food Engineering,* 13(8), 20160271. doi:https://doi.org/10.1515/ijfe-2016-0271

Nguyen, T. T. T., Nguyen, V. B., and Kha, T. C. (2025). Optimization of bioactive compounds extraction from *Red Cardinal* grape pomace using choline chloride and lactic acid-based deep eutectic solvent. *Preparative Biochemistry & Biotechnology*, 1-12. doi:https://doi.org/10.1080/10826068.2025.2465960

Pajareon, S., and Theerakulkait, C. (2017). Effects of spray drying at different inlet air temperatures on antioxidative activity and some properties of Homnil rice bran extract powder. *Pakistan Journal of Nutrition,* 16(10), 782-788. doi:https://doi.org/10.3923/pjn.2017.782.788

Peixoto, C. M., Dias, M. I., Alves, M. J., Calhelha, R. C., Barros, L., Pinho, S. P., and Ferreira, I. C. (2018). Grape pomace as a source of phenolic compounds and diverse bioactive properties. *Food Chemistry,* 253, 132-138. doi:https://doi.org/10.1016/j.foodchem.2018.01.163

Perković, G., Planinić, M., Šelo, G., Martinović, J., Nedić, R., Puš, M., and Bucić-Kojić, A. (2024). Optimisation of the encapsulation of grape pomace extract by spray drying using goat whey protein as a coating material. *Coatings,* 14(9), 1101. doi:https://doi.org/10.3390/coatings14091101

Qi, P. X., and Onwulata, C. I. (2011). Physical properties, molecular structures, and protein quality of texturized whey protein isolate:

Effect of extrusion temperature. *Journal of Agricultural and Food Chemistry,* 59(9), 4668-4675. doi:https://dx.doi.org/10.1021/jf2011744

Romano, A., Masia, P., Puccia, E., Oliviero, V., and Ferranti, P. (2017). Encapsulated proanthocyanidins as novel ingredients. *Chemical Engineering Transactions,* 57, 1885-1890. doi:https://doi.org/10.3303/CET1757315

Rosenberg, M., Rosenberg, Y., and Frenkel, L. (2016). Microencapsulation of model oil in wall matrices consisting of SPI and maltodextrins. *AIMS Agriculture and Food,* 1(1), 33-51. doi:https://doi.org/10.3934/agrfood.2016.1.33

Ruprecht, N., Liebig, L., Hajare, V., and Kohlus, R. (2022). *Thermal Damages in Spray drying-Effect of Particle Size and Residence Time Ratio.* Paper presented at the Proceedings of the 22nd International Drying Symposium on Drying Technology-IDS, Worcester, Massachusetts, USA.

Shi, Q., Fang, Z., and Bhandari, B. (2013). Effect of addition of whey protein isolate on spray-drying behavior of honey with maltodextrin as a carrier material. *Drying Technology,* 31(13-14), 1681-1692. doi:https://doi.org/10.1080/07373937.2013.783593

Škulcova, A., Haščičová, Z., Hrdlička, L., Šima, J., and Jablonský, M. (2018). Green solvents based on choline chloride for the extraction of spruce bark (Picea abies). *Cellulose Chemistry and Technology,* 52(3-4), 171-179.

Tan, S. P., Vuong, Q. V., Stathopoulos, C. E., Parks, S. E., and Roach, P. D. (2014). Optimized aqueous extraction of saponins from bitter melon for production of a saponin-enriched bitter melon powder. *Journal of Food Science,* 79(7), E1372-E1381. doi:https://doi.org/10.1111/1750-3841.12514

Tolun, A., Altintas, Z., and Artik, N. (2016). Microencapsulation of grape polyphenols using maltodextrin and gum arabic as two alternative coating materials: Development and characterization. *Journal of Biotechnology,* 239, 23-33. doi:https://doi.org/10.1016/j.jbiotec.2016.10.001

Ton, N. M. N., and Dao, V. H. (2006). Application of spray drying in passion fruit powder production. *VNUHCM Journal of Science and Technology Development,* 9(4). doi:https://doi.org/10.32508/stdj.v9i4.2903

Tuyen, C. K., Nguyen, M. H., and Roach, P. D. (2010). Effects of spray drying conditions on the physicochemical and antioxidant properties of the Gac (*Momordica cochinchinensis*) fruit aril powder. *Journal of Food Engineering,* 98(3), 385-392. doi:https://doi.org/10.1016/j.jfoodeng.2010.01.016

Vincken, J.-P., Heng, L., de Groot, A., and Gruppen, H. (2007). Saponins, classification and occurrence in the plant kingdom. *Phytochemistry,* 68(3), 275-297. doi:https://doi.org/10.1016/j.phytochem.2006.10.008

Vu, A. T., Kha, T. C., and Phan, H. T. (2023). Encapsulation of bioactive compounds from germinated mung bean by freeze-drying, release kinetics, and storage stability. *Foods,* 13(1), 100. doi:https://doi.org/10.3390/foods13010100

Wang, X., Ding, Z., Zhao, Y., Prakash, S., Liu, W., Han, J., and Wang, Z. (2021). Effects of lutein particle size in embedding emulsions on encapsulation efficiency, storage stability, and dissolution rate of microencapsules through spray drying. *LWT,* 146, 111430. doi:https://doi.org/10.1016/j.lwt.2021.111430

Xiao, Z., Xia, J., Zhao, Q., Niu, Y., and Zhao, D. (2022). Maltodextrin as wall material for microcapsules: A review. *Carbohydrate Polymers,* 298, 120113. doi:https://doi.org/10.1016/j.carbpol.2022.120113

Yao, H., Liu, B., He, L., Hu, J., and Liu, H. (2023). The incorporation of peach gum polysaccharide into soy protein based microparticles improves probiotic bacterial survival during simulated gastrointestinal

digestion and storage. *Food Chemistry,* 413, 135596. doi:https://doi.org/10.1016/j.foodchem.2023.135596

Acknowledgments

This research was funded by Nong Lam University, Ho Chi Minh City, Vietnam, grant number CS-CB25-HHTP-03. The authors would like to thank Ba Moi Company for supplying grape pomace.